Syngeneic natural killer cell therapy activates dendritic and T cells in metastatic lungs and effectively treats low-burden metastases

Shih-Wen Huang[1,2,#], Yein-Gei Lai[1,#], Hao-Ting Liao[1,3,#], Chin-Ling Chang[1], Ruo-Yu Ma[1], Yung-Hsiang Chen[1], Yae-Huei Liou[1], Zhen-Qi Wu[1], Yu-Chen Wu[4], Ko-Jiunn Liu[4], Yen-Tsung Huang[5], Jen-Lung Yang[1], Ming-Shen Dai[6*], and Nan-Shih Liao[1,2*]

[1]Institute of Molecular Biology, Academia Sinica, Taipei, Taiwan

[2]Molecular and Cell Biology, Taiwan International Graduate Program, Academia Sinica and Graduate Institute of Life Science, National Defense Medical Center, Taipei, Taiwan

[3]Department of Life Sciences, National Central University, Taoyuan, Taiwan

[4]National Institute of Cancer Research, National Health Research Institutes, Tainan, Taiwan

[5]Institute of Statistical Science, Academia Sinica, Taipei, Taiwan

[6]Department of Hematology-Oncology, Tri-Service General Hospital, Taipei, Taiwan

[#]Co-first authors, *Co-corresponding authors

Abstract

Natural killer (NK) cells can control metastasis through cytotoxicity and IFN-γ production independently of T cells in experimental metastasis mouse models. The inverse correlation between NK activity and metastasis incidence supports a critical role for NK cells in human metastatic surveillance. However, autologous NK cell therapy has shown limited benefit in treating patients with metastatic solid tumors. Using a spontaneous metastasis mouse model of MHC-I^{+} breast cancer, we found that transfer of IL-15/IL-12-conditioned syngeneic NK cells after primary tumor resection promoted long-term survival of mice with low metastatic burden and induced a tumor-specific protective T cell response that is essential for the therapeutic effect. Furthermore, NK cell transfer augments activation of conventional dendritic cells (cDCs), Foxp3^{-}CD4^{+} T cells and stem cell-like CD8^{+} T cells in metastatic lungs, to which IFN-γ of the transferred NK cells contributes significantly. These results imply direct interactions between transferred NK cells and endogenous cDCs to enhance T cell activation. We conducted an investigator-initiated clinical trial of autologous NK cell therapy in six patients with advanced cancer and observed that the NK cell therapy was safe and showed signs of effectiveness. These findings indicate that autologous NK cell therapy is effective in treating established low burden metastases of MHC-I^{+} tumor cells by activating the cDC-T cell axis at metastatic sites.

35 **Introduction**

36

37 Metastasis is the most common cause of cancer death, and effective therapies for established
38 metastases are currently lacking (Ganesh & Massague, 2021). Natural killer (NK) cells play a
39 critical role in metastasis control, as the abundance of functional circulating or tumor-
40 infiltrating NK cells is inversely correlated with metastasis incidence while being positively
41 correlated with favorable prognoses for patients with or at risk of metastasis (Lopez-Soto,
42 Gonzalez, Smyth, & Galluzzi, 2017). NK cells are capable of recognizing tumor cells via
43 various activating and inhibitory NK receptors (NKRs). Tumor cells often down-regulate the
44 expression of ligands for inhibitory NKRs, yet express stress-induced ligands for activating
45 NKRs. Upon encountering tumor cells, the reduced inhibitory NKR engagement and
46 enhanced activating NKR engagement facilitate NK cell activation (Jamieson et al., 2002;
47 Karre, Ljunggren, Piontek, & Kiessling, 2005). NK cells also express receptors for activating
48 cytokines, such as IL-15, IL-12, IL-18 and IL-21, as well as receptors for suppressive factors
49 such as TGF-β and prostaglandin E2 present in the tumor microenvironment (Huntington,
50 Cursons, & Rautela, 2020). The sum of signals transduced through the activating and
51 inhibitory receptors determines NK cell activation. Activated NK cells kill engaged tumor
52 cells via perforin, granzymes, and the death receptor ligands TNF-α, TRAIL and FasL
53 (Smyth et al., 2005). Activated NK cells also produce IFN-γ, which directly inhibits tumor
54 cell growth and induces type 1 T helper cell (T_H1) and cytotoxic $CD8^+$ T cell responses that
55 are critical for effective anti-tumor immunity (Alspach, Lussier, & Schreiber, 2019; Martin-
56 Fontecha et al., 2004). Moreover, intratumoral NK cells produce XCL1 and CCL5 to recruit
57 type 1 conventional dendritic cells (cDC1) that cross-present cell-associated tumor antigen to
58 $CD8^+$ T cells (Bottcher et al., 2018), and also produce Flt3L to increase the abundance of
59 cDCs (Barry et al., 2018). However, the immunosuppressive microenvironment induced by

60 tumor cells elicits NK cell and T cell dysfunction (Melaiu, Lucarini, Cifaldi, & Fruci, 2019;
61 Thommen & Schumacher, 2018).
62
63 Two anti-metastatic mechanisms of NK cells have been revealed to date, i.e., cytotoxicity and
64 IFN-γ production. In the metastatic cascade, the epithelial-mesenchymal transition increases
65 the susceptibility of tumor cells to NK cell cytotoxicity by modulating the expression of
66 ligands for the activating NKRs NKG2D (Lopez-Soto et al., 2013), E-cadherin and cell
67 adhesion molecule 1 (Chockley et al., 2018), as well as MHC class I (MHC-I) molecules
68 (Chen et al., 2015). The IFN-γ produced by NK cells was shown to be essential for natural
69 resistance to lung metastasis in a B16 melanoma model (Takeda et al., 2011) and for the IL-
70 12-mediated suppression of liver metastasis in a CT-26 model (Uemura et al., 2010) using
71 *Rag* knockout mice that lacked T cells. Another study indicated that the anti-metastasis effect
72 of IL-12 produced by Baft3-dependent DCs is mediated through IFN-γ production by NK
73 cells without the involvement of T cells (Mittal et al., 2017). NK cells also sustain the
74 dormancy of metastatic tumor cells seeded in distal organs through cytotoxicity and IFN-
75 γ (Correia et al., 2021; Malladi et al., 2016). The anti-metastatic mechanisms described above
76 do not involve T cells. Thus, whether T cell immunity plays a role in the anti-metastatic
77 function of NK cells remains to be elucidated.
78
79 Despite the clear anti-tumor function of endogenous NK cells, adoptive transfer of ex vivo-
80 expanded autologous NK cells has shown limited clinical benefit in treating patients with
81 metastatic or locally advanced solid tumors, including melanoma, renal cell carcinoma, and
82 digestive cancer (Parkhurst, Riley, Dudley, & Rosenberg, 2011; Sakamoto et al., 2015). Both
83 the immunosuppressive microenvironment induced by tumor cells (Melaiu et al., 2019) and
84 heterogeneity of NK cell subpopulations and their respective functions (Freud, Mundy-Bosse,

85 Yu, & Caligiuri, 2017) likely contribute to this therapeutic limitation. Given the vast array of
86 approaches used for ex vivo expansion of NK cells (Fang, Xiao, & Tian, 2017), different
87 methods may result in NK cells exerting different functions. We hypothesize that autologous
88 NK cells with anti-tumor activities are effective in treating low burden metastases. In this
89 study, we used syngeneic IL-15/IL-12-conditioned NK cells to treat established lung
90 metastases after resection of the primary MHC-I$^+$ EO771 mammary tumor. We found that the
91 NK cell therapy promoted long-term survival of mice with low metastatic burden in a CD8$^+$
92 T cell-dependent manner, and induced tumor-specific protective immune memory.
93 Furthermore, NK cell transfer augmented the activation of cDC1, cDC2 and T cells in
94 metastatic lungs, which requires IFN-γ of the transferred NK cells. We also conducted an
95 investigator-driven clinical trial of autologous NK cell therapy on six patients hosting four
96 cancer types and found that the therapy is safe and shows signs of efficacy.
97
98
99 **Results**
100
101 **Characterization of ex vivo-expanded murine NK cells**
102 To generate NK cells with anti-tumor activity ex vivo, we cultured murine BM cells with IL-
103 15 and IL-12, since IL-15 is an NK cell growth and survival factor and both cytokines
104 enhance IFN-γ production and the cytotoxicity of NK cells (Kennedy et al., 2000; Lodolce et
105 al., 1998; Marcenaro et al., 2005). On average, 86% of the resulting cells were identified as
106 TCRαβ$^-$TCRγδ$^-$CD19$^-$NK1.1$^+$ that express NKG2D, EOMES and T-bet (Figure 1A),
107 representing characteristics of NK cells (Gordon et al., 2012; Raulet, 2003). Approximately
108 90% of the expanded NK cells were CD27$^+$ with no-to-low levels of CD11b expression
109 (Figure 1A). The proportion of NK cells expressing MHC-I-interacting NKRs, including

110 activating Ly49D/H and inhibitory Ly49A/G2/I and NKG2A, was stable among independent
111 cultures (Figure 1B). In terms of activation status, on average, 87% of the expanded NK cells
112 expressed either intermediate or high levels of the activating receptor DNAM-1 and 82% of
113 them displayed an activated $B220^{+}CD11c^{+}$ phenotype (Figure 1C). Consistently, they
114 expressed the anti-tumor effectors IFN-γ, granzyme B, and TRAIL (Figure 1D). Co-culturing
115 the NK cells with either EO771 breast adenocarcinoma cells that express MHC-I molecules
116 and Rae-1 or B16F10 melanoma cells that express none of those molecules in vitro (Figure 1-
117 figure supplement 1) resulted in dose-dependent tumor cell death (Figure 1E) and up-
118 regulation of IFN-γ production by the NK cells (Figure 1F). Thus, the NK cells conditioned
119 by means of IL-15 and IL-12 possess anti-tumor activities in vitro.

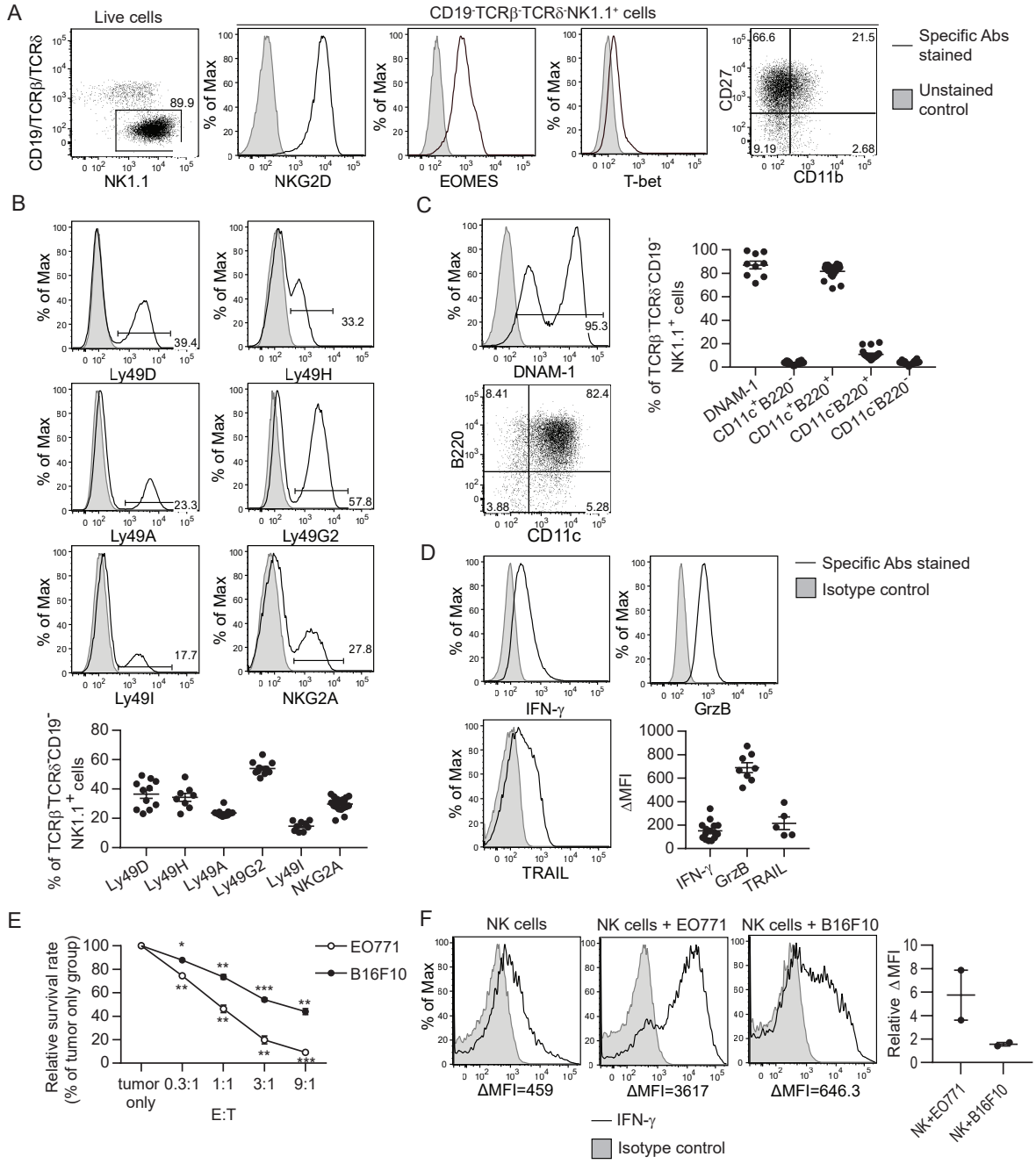

Figure 1. Characterization of ex vivo-expanded murine NK cells.

BM cells were cultured with IL-15 and IL-12 as described in Methods. (A) Analysis of NK cells (CD19⁻ TCRαβ⁻TCRγδ⁻NK1.1⁺) among live expanded cells. Plots are representative of 20 independent cultures. (B)-(D) Expression of MHC-I-interacting activating and inhibitory NKRs, activation markers and anti-tumor effectors by the expanded NK cells. Representative flow histograms are presented for each molecule, and the compiled data from independent expansion cultures is indicated by the dot plots. (E) In vitro cytotoxicity of the expanded NK cells. CFSE-labeled EO771 or B16F10 cells (T, target) were co-cultured with expanded NK cells (E, effector) at the indicated E:T ratios. Tumor cell viability was analyzed by PI staining using FACS. One representative of three independent experiments is shown. Data represent mean ± SEM of triplicate wells. Statistical significance was determined by unpaired two-tailed Student's t-test: *$P<0.05$, **$P<0.01$, ***$P<0.001$

132 relative to tumor only. (F) Tumor cells stimulated IFN-γ production by the expanded NK cells. Sorted NK cells
133 were cultured alone (NK cells) or together with indicated tumor cells at a ratio of 1:1. Levels of intracellular
134 IFN-γ of NK cells were determined by staining with anti-IFN-γ or isotype control antibody, and analyzed by
135 FACS. Representative histograms from one of two independent experiments and the relative difference in mean
136 fluorescence intensity (ΔMFI) of the two experiments are shown. ΔMFI was calculated by subtracting the MFI
137 value of isotype control staining from that of anti-IFN-γ antibody staining. Relative ΔMFI was calculated by
138 dividing the ΔMFI of NK cells + tumor cells with the ΔMFI of NK cells.
139 **Figure supplement 1.** Expression of MHC-I molecules and Rae-1 by EO771 and B16F10 cells *in vitro*.

140 **EO771 tumor-resected mice represent a model for established metastases to test NK cell**
141 **therapy**

142 Cancer recurrence occurs in a significant proportion of patients after primary tumor resection
143 due to dissemination of tumor cells before and/or during surgery. To mimic that scenario, we
144 established a syngeneic orthotopic breast cancer model using the MHC-I$^+$ EO771 cell line
145 that harbors numerous mutations (Y. Yang et al., 2017). At 21 days post-inoculation and
146 consistent with the spontaneous lung metastatic property of the EO771 line (Ewens, Mihich,
147 & Ehrke, 2005), we observed that ~85% of mice with a primary tumor weighing ≥ 95 mg had
148 metastatic foci on the lung surface. The number and area of metastatic foci was positively
149 correlated with tumor weight on day 21 (Figure 2A). Resection of the primary tumor and its
150 sentinel lymph node (LN) on day 21 resulted in a long-term survival rate of 18%, with
151 mortality of all remaining mice (Figure 2B). All dead mice exhibited metastases in the lung,
152 of which 71% displayed tumor reappearance at the surgical site (data not shown). Therefore,
153 this tumor resection model represents a model of established metastases caused by tumor cell
154 dissemination before and arising from surgery. To apply adoptive NK cell therapy to this
155 model, we examined if the transferred NK cells reach the lungs of tumor-resected mice. The
156 expanded NK cells express the chemokine receptors CXCR3, CCR5 and CXCR6 (Figure 2C),
157 and the lung of tumor-resected mice express mRNA of the corresponding ligands
158 CXCL9/10/11, CCL3/4/5 and CXCL16 (Figure 2D). Using eGFP$^+$ NK cells, we observed
159 that numbers of transferred cells in the lung peaked at 4 h and then continuously declined,
160 remaining detectable for at least 2 days (Figure 2E). A similar pattern of transferred NK cells
161 was observed in the spleen, albeit with lower cell counts (Figure 2E).

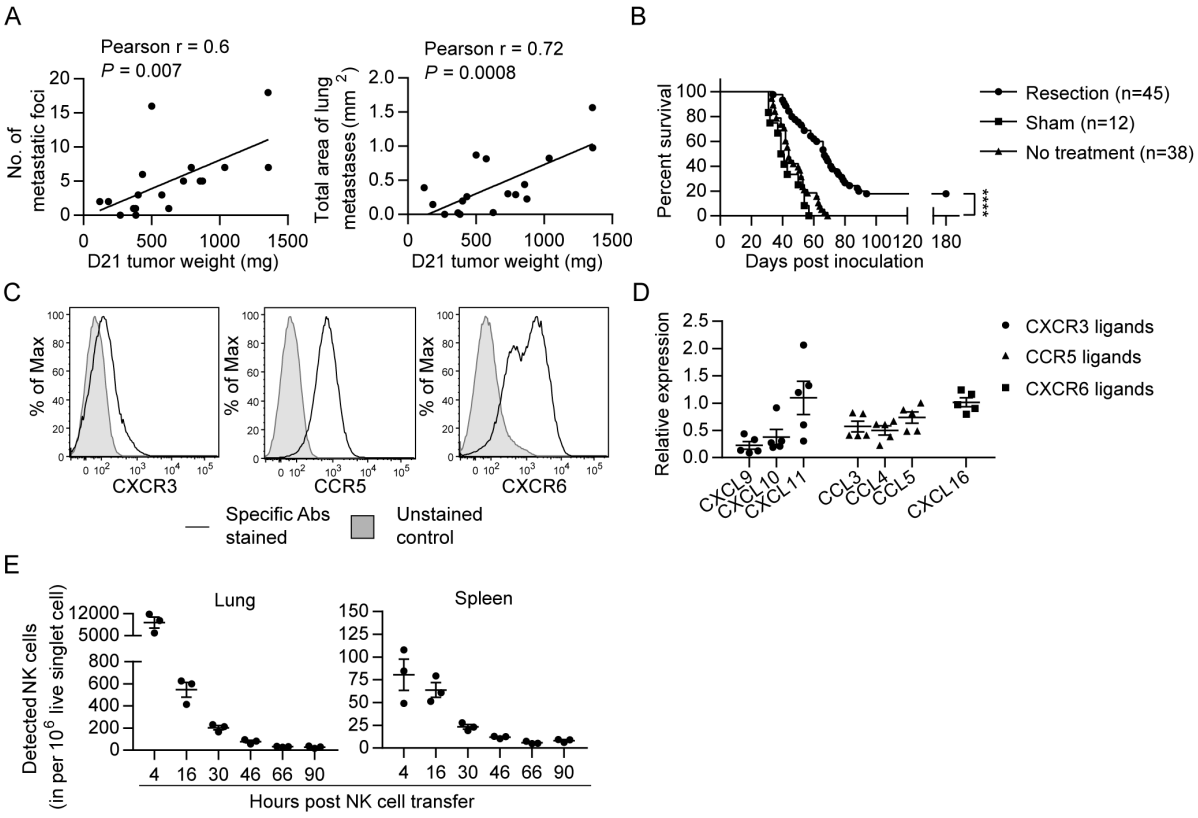

Figure 2. EO771 tumor resection and metastasis model for NK cell treatment**.**

(A) Positive correlation between primary tumor weight and lung metastasis. Pearson correlations between day 21 tumor weights and the number and total area of metastatic foci on the lung surface are shown. Each dot represents a mouse. (B) Survival of mice who received day 21 tumor resection, sham surgery, or no treatment. Mouse survival was analyzed by means of the Kaplan-Meier estimator and a Log-Rank test: ****P<0.0001. (C) Expanded NK cells express the chemokine receptors CXCR3, CCR5 and CXCR6. Representative flow plots of 10 independent cultures are shown. (D) Expression of CXCR3, CCR5 and CXCR6 ligands in the lung. Specific gene expression was determined by quantitative real-time PCR using lung RNA of day 21 tumor-resected mice collected on day 24 post tumor inoculation and normalized to the expression of cyclophilin a. Each symbol represents a mouse and means ± SEM are shown. (E) Expanded eGFP$^+$ NK cells were transferred into day 21 EO771-resected mice on day 24, and quantified in the single cell suspensions of spleen and lung at the indicated times using FACS. Numbers of eGFP$^+$ NK cells detected in each organ are shown. Each dot represents a mouse (means ± SEM).

177 **Syngeneic NK cell therapy is effective in treating mice with low metastatic burden in a**
178 **$CD8^+$-T-cell-dependent manner**
179 We evaluated the effect of syngeneic NK cell therapy on tumor-resected mice (Figure 3A
180 Schema), and found a negative correlation between survival time and day 21 tumor weight in
181 the NK cell-treated group but not in the control group (Figure 3A). Consequently, we divided
182 the mice into two groups according to their day 21 tumor weight. NK cell-treated mice
183 displayed significantly enhanced overall survival (OS) and an improved long-term survival
184 rate from 33% to 68% compared to control mice in the 95-400 mg tumor group, whereas the
185 same therapy did not improve OS of the > 400 mg tumor group (Figure 3B). These results,
186 together with the result presented in Figure 2A, indicate that the NK cell therapy promotes
187 long-term survival of tumor-resected mice carrying low metastatic burden. We further
188 examined if the surviving mice after NK cell treatment had acquired tumor-specific
189 protection by re-challenging them with either EO771 or B16F10 tumor cells (Figure 3C
190 Schema). We found that 83% of these mice were protected from EO771 re-challenge and
191 survived beyond 180 days, whereas all mice re-challenged with B16F10 died (Figure 3C).
192 Age-matched naïve mice inoculated for the first time with either EO771 or B16F10 as a
193 control all died (Figure 3C). Thus, surviving mice of post-resection NK cell therapy
194 displayed tumor-specific protective immunity.
195
196 Since the tumor re-challenge experiment was performed at 11-13 weeks following NK cell
197 treatment (Figure 3C), the observed long-lasting protection is likely mediated by memory T
198 cells. Accordingly, we examined the role of T cells in NK cell therapy by depleting T cell
199 subsets with anti-CD4 or/and anti-CD8 antibodies two days before primary tumor resection
200 (Figure 3D Schema and Figure 3-figure supplement 1). In the 95-600 mg tumor group,
201 depletion of $CD8^+$ cells alone or both $CD4^+$ and $CD8^+$ cells diminished the effect of NK cell

202 therapy, whereas depletion of $CD4^+$ cells alone did not affect OS (Figure 3D). This result
203 indicates that $CD8^+$ T cells are essential for the effect of NK cell therapy. In contrast, the
204 >600 mg tumor group displayed a limited NK cell treatment effect as expected, but did
205 exhibit an improvement in OS upon depleting $CD4^+$ cells alone (Figure 3D). As the
206 proportion of lung $Foxp3^+CD4^+$ T cells in $CD45^+$ cells positively correlated with day 21
207 tumor weight (data not shown), depletion of $Foxp3^+CD4^+$ T cells by anti-CD4 antibody likely
208 has a stronger effect in augmenting the immune response for the >600 mg tumor than the 95-
209 600 mg tumor group. Moreover, both tumor groups showed diminished OS upon depletion of
210 both $CD4^+$ and $CD8^+$ cells than was the case for depletion of $CD8^+$ cells alone, indicating a
211 $CD8^+$ T cell-independent anti-tumor effect of $CD4^+$ T cells (Figure 3D).
212
213 Next, we examined whether the T cells in surviving mice after NK cell therapy and tumor re-
214 challenge possess anti-tumor activity. T cells and non-T cells were isolated from individual
215 NK cell-treated and EO771-rechallenged survivors or from age-matched donors, and then
216 transferred into naïve recipients in a 1-donor-to-1-recipient manner. The recipient mice were
217 inoculated with EO771 cells to evaluate the anti-tumor effects of the donor cells, whereas
218 naïve mice received no donor cells and served as a control for tumor growth (Figure 3E
219 Schema). For the mice receiving cells isolated from the survivors, 5 of 6 T-cell recipients and
220 1 of 6 non-T-cell recipients survived beyond 120 days post tumor inoculation (Figure 3E). In
221 contrast, mice receiving either T or non-T cells isolated from age-matched naïve donors all
222 died. Mice that received no donor cells in both experiments also all died (Figure 3E).
223 Together, these results indicate that the post-resection NK cell therapy induces a tumor-
224 specific T cell response with memory that is essential for its treatment efficacy.

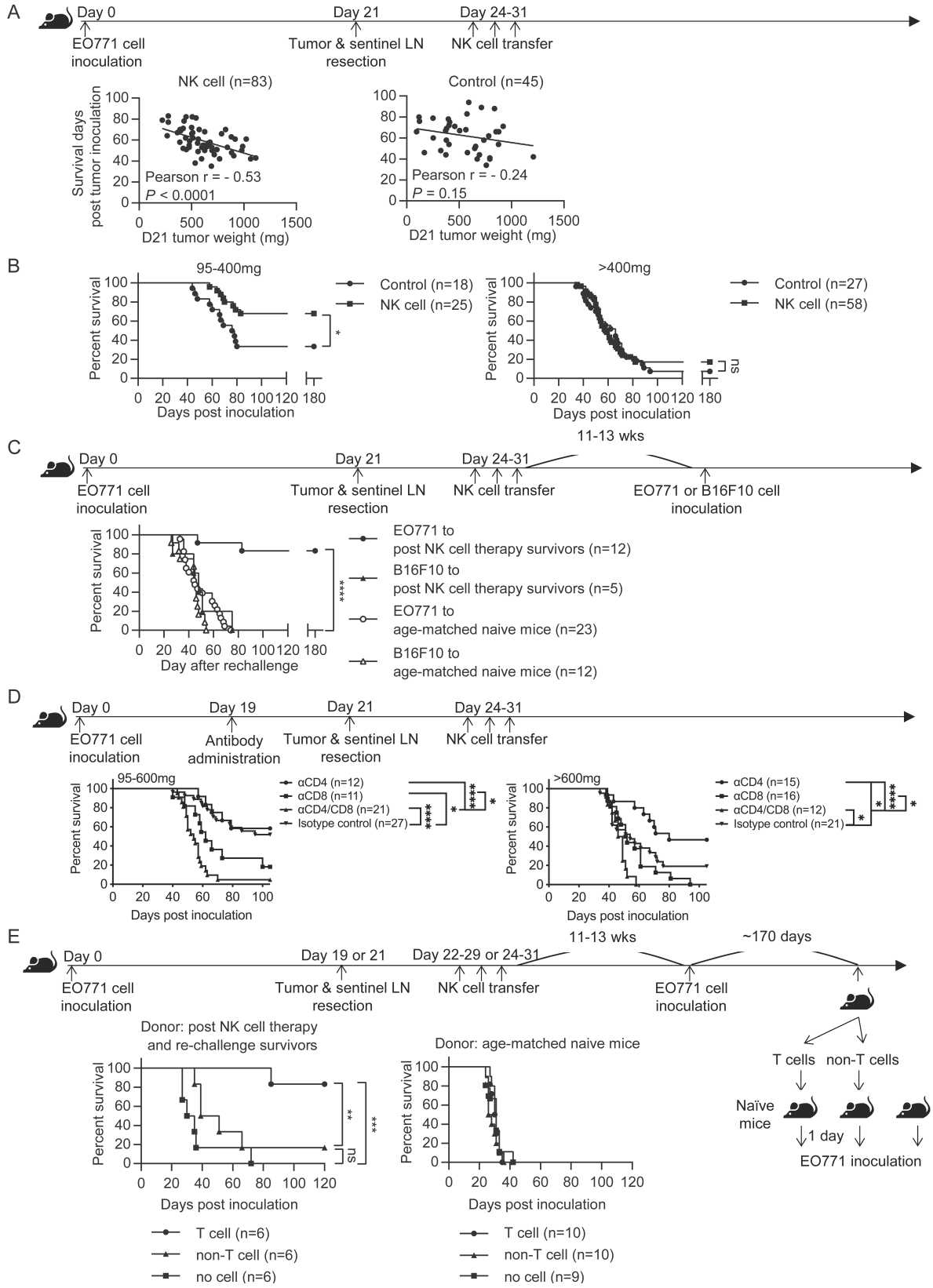

Figure 3. Syngeneic NK cell therapy is effective in treating mice with low metastatic burden in a CD8$^+$-T-cell-dependent manner.

(A) Day 21 tumor weight is inversely correlated with survival duration of NK-cell-treated tumor-resected mice. After tumor and sentinel LN resection on day 21, mice received either sorted NK cells (NK cell) or PBS

231 (Control) at the indicated time-points. The correlation between day 21 tumor weight and survival time of mice
232 was evaluated by Pearson correlation. Each dot represents a mouse. The results have been compiled from 5-8
233 independent experiments. The Control group is the same dataset as presented for the Resection group in Figure
234 2B. (B) NK cell therapy promotes long-term survival of mice who had light tumors on day 21. The mice
235 described in (A) were separated into 95-400 mg and >400 mg day 21 tumor weight groups for survival analysis
236 by means of the Kaplan-Meier estimator and a Log-Rank test: *P<0.05. (C) NK cell therapy induces tumor-
237 specific protection. Surviving mice after NK cell therapy were re-challenged with EO771 (●, compiled from
238 four independent experiments) or B16F10 cells (▲, compiled from two independent experiments) at 11-13
239 weeks post therapy, and then monitored for survival. Age-matched naïve mice were inoculated with EO771 (○,
240 compiled from four independent experiments) or B16F10 cells (△, compiled from three independent
241 experiments) as controls. Mouse survival, using 2000 mm^3 tumor volume as a cut-off, was analyzed by means
242 of the Kaplan-Meier estimator and a Log-Rank test: ****P<0.001. (D) Depletion of $CD4^+$ or/and $CD8^+$ cells
243 alters the effects of NK cell therapy. Mice were treated with indicated antibodies at day 19 post tumor
244 inoculation, and then received resection followed by NK cell therapy. Mice were grouped according to indicated
245 primary tumor weight for survival analysis by means of the Kaplan-Meier estimator and a Log-Rank test: ns,
246 not significant; *P<0.05; ***P<0.001; ****P<0.0001. The data are compiled from 2-3 experiments. (E) T cells
247 isolated from surviving mice post NK cell therapy and tumor re-challenge confer anti-tumor activity. Post NK
248 cell therapy and re-challenge survivors were collected from three independent experiments. T cells and non-T
249 cells isolated from each survivor were transferred separately into naïve recipient mice in a 1-donor-to-1-
250 recipient manner, whereas other naïve mice that received no cells served as a control (compiled from two
251 independent experiments). T cells and non-T cells were also isolated from age-matched naïve donors and
252 transferred separately into naïve recipient mice, whereas other naïve mice that received no cells served as a
253 control (compiled from two independent experiments). The recipient mice were then inoculated with EO771
254 cells one day after cell transfer. Mouse survival, using 2000 mm^3 tumor volume as a cut-off, was analyzed by
255 means of the Kaplan-Meier estimator and a Log-rank test: ns, not significant; **P<0.01; ***P<0.001.
256 **Figure supplement 1.** Effectiveness of in vivo depletion of $CD4^+$ and $CD8^+$ T cells by antibody (related to
257 Figure 3D).

258 **Syngeneic NK cell transfer promotes cDC and T cell activation in metastatic lungs**

259 Conventional DCs directly trigger an antigen-specific T cell response by providing ligands to
260 antigen, costimulatory and cytokine receptors expressed on T cells (Cabeza-Cabrerizo,
261 Cardoso, Minutti, Pereira da Costa, & Reis e Sousa, 2021). A previous in vivo study reported
262 that A20 lymphoma expressing abnormally low levels of MHC I molecules (MHC-I) induces
263 IL-12 production by splenic DCs ($CD11c^{+}CD19^{-}F4/80^{-}$) and $CD8^{+}$ T cell response (Mocikat
264 et al., 2003). Therefore, we hypothesized that our NK cell therapy would modulate cDCs in
265 metastatic lungs in favor of a T cell response. As our IL-15/IL-12-conditioned NK cells
266 express high levels of mRNA encoding IFN-γ and IL-10 (data not shown), cytokines known
267 to modulate cDC function, we examined whether one transfer of wild type (WT), *Il10*$^{-/-}$ or
268 *Ifng*$^{-/-}$ NK cells affected cDCs and T cells in the metastatic lungs. Immune cells were
269 analyzed ~18 hours after NK-cell transfer, by which time the level of transferred NK cells in
270 the lung declined by > 60% relative to that determined at 4-hours (Fig. 2E). We found that
271 lung cDC1s and cDC2s consist of cells expressing either high or low level of MHC-II (MHC-
272 II^{hi} or MHC-II^{lo}), and the MHC-II^{hi} cDCs are composed of $CCR7^{+}Lamp3^{+}$ and $CCR7^{-}Lamp3^{-}$
273 subsets (Figure 4A). The $CCR7^{+}Lamp3^{+}$MHC-II^{hi} subset expresses the highest level of APC
274 function molecules, including MHC-I, MHC-II, CCR7, CD86, CD40 and PD-L1 (Figure 4A),
275 resembling the recently identified mregDC (Cheng et al., 2021; de Saint-Vis et al., 1998;
276 Maier et al., 2020). The $CCR7^{-}Lamp3^{-}$MHC-II^{hi} subset expresses an intermediate level of
277 MHC-II, CD86 and CD40 among the three subsets, and similar levels of MHC-I, CCR7 and
278 PD-L1 to that of the MHC-II^{lo} subset (Figure 4A). NK-cell transfer did not alter the
279 proportion of total cDC1s or cDC2s in $CD45^{+}$ cells in the lung tissue (data not show).
280 However, among cDC1s, transfer of WT NK cells significantly increased the proportion of
281 the two MHC-II^{hi} subsets, the levels of CD86 and CD40 expressed by all three subsets, and
282 the levels of PD-L1, MHC-I and MHC-II expressed by $CCR7^{-}Lamp3^{-}$MHC-II^{hi} and MHC-II^{lo}

283 subsets (Figure 4B). IFN-γ, but not IL-10, of the transferred NK cells significantly
284 contributes to these effects, except for the PD-L1 level in MHC-II^{lo} subset (Figure 4B).
285 Transfer of WT NK cells exerted many effects on cDC2s similar to those described above for
286 cDC1s, albeit with several differences (Figure 4B). The differences include augmenting
287 MHC-II level in the CCR7^{+}Lamp3^{+}MHC-II^{hi} subset, reducing MHC-II level in the MHC-II^{lo}
288 subset, and having no effect on CD40 level in the CCR7^{+}Lamp3^{+}MHC-II^{hi} subset (Figure
289 4B). IFN-γ of transferred NK cells significantly contributed to these effects of WT NK cell
290 transfer on cDC2s, except for the increase of the CCR7^{+}Lamp3^{+}MHC-II^{hi} subset, CD40 and
291 MHC-II levels in the CCR7^{-}Lamp3^{-}MHC-II^{hi} subset, and CD86 and MHC-II levels in the
292 MHC-II^{lo} subset (Figure 4B).

A

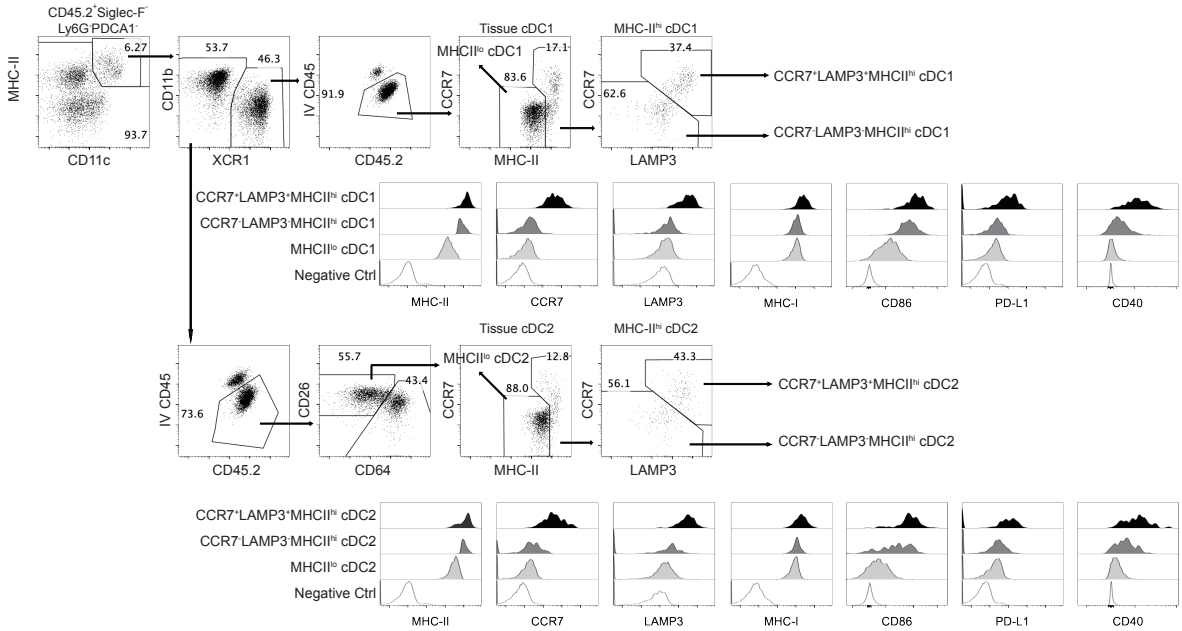
CD45.2+Siglec-F-
Ly6G-PDCA1-
MHC-II
CD11c
6.27
93.7
CD11b
XCR1
53.7
46.3
IV CD45
CD45.2
91.9
Tissue cDC1
MHCIIlo cDC1
CCR7
MHC-II
17.1
83.6
MHC-IIhi cDC1
CCR7
LAMP3
37.4
62.6
CCR7+LAMP3+MHCIIhi cDC1
CCR7-LAMP3-MHCIIhi cDC1
CCR7+LAMP3+MHCIIhi cDC1
CCR7-LAMP3-MHCIIhi cDC1
MHCIIlo cDC1
Negative Ctrl
MHC-II
CCR7
LAMP3
MHC-I
CD86
PD-L1
CD40
IV CD45
CD45.2
73.6
CD26
CD64
55.7
43.4
Tissue cDC2
MHCIIlo cDC2
CCR7
MHC-II
12.8
88.0
MHC-IIhi cDC2
CCR7
LAMP3
43.3
56.1
CCR7+LAMP3+MHCIIhi cDC2
CCR7-LAMP3-MHCIIhi cDC2
CCR7+LAMP3+MHCIIhi cDC2
CCR7-LAMP3-MHCIIhi cDC2
MHCIIlo cDC2
Negative Ctrl
MHC-II
CCR7
LAMP3
MHC-I
CD86
PD-L1
CD40

293

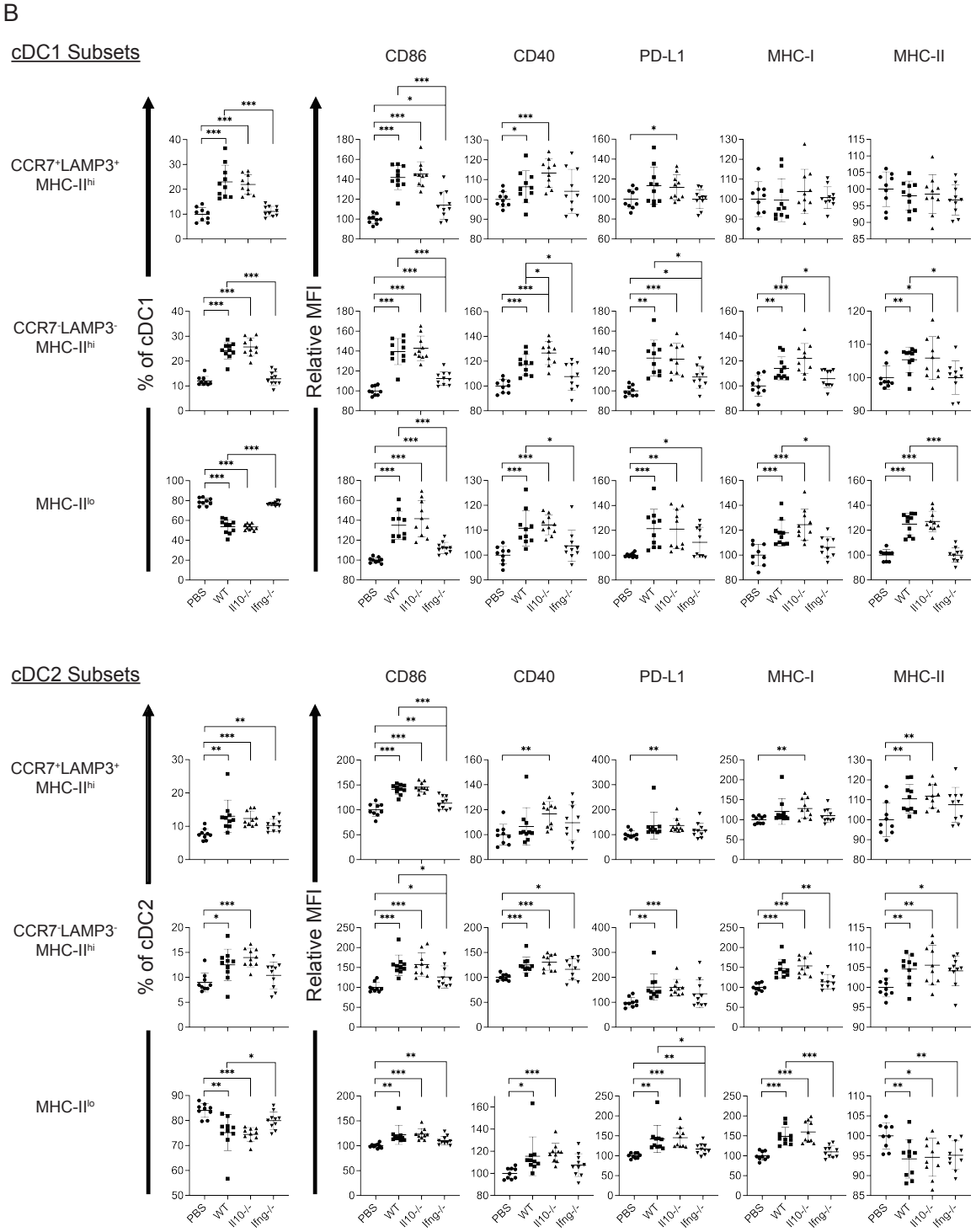

Figure 4. Syngeneic NK cell transfer modulates APC function of cDC in the metastatic lungs. The experimental design is the same as depicted in the Fig. 3A schema except that NK cells (WT, *Il10*$^{-/-}$ or *Ifng*$^{-/-}$) were transferred once on day 24 and lung immune cells were analyzed on day 25. (A) Gating strategies and characterization of cDC subsets in lung tissue. The dot plots show the gating of CCR7^{+}LAMP3^{+}MHC-II^{hi}, CCR7^{-}LAMP3^{-}MHC-II^{hi} and MHC-II^{lo} subsets of cDC1s and cDC2s. The histograms show the comparison of indicated molecules expressed by the three subsets of cDC1s and cDC2s. Negative controls are either fluorescence-minus-one (FMO) or single stain of another molecule. Data shown are from a representative PBS-

303 treated mouse. (B) NK-cell transfer affects the activation of lung cDCs. The proportion of the three cDC subsets
304 in cDC1s and cDC2s are shown. The expression of the indicated APC function molecules was analyzed as
305 relative MFI, based on normalization against the mean MFI of the PBS group in each independent experiment.
306 Data are compiled from two independent experiments and presented as mean ± SEM. Each symbol represents
307 one mouse. Statistical significance was determined by unpaired two-tailed Student's t-test: *P≤0.05, **P≤0.01,
308 ***P≤0.001.

309 Next, we examined T cells in the lung tissue. Transfer of WT NK cells increased the
310 proportion of Foxp3$^-$CD4$^+$ and CD8$^+$ T cells without altering that of Foxp3$^+$CD4$^+$ T cells
311 (Figure 5A and Figure 5-figure supplement 1A). The proportion of activated Foxp3$^-$CD4$^+$ T
312 cells, including effector (CD62L$^-$CD44$^+$), PD-1$^+$ and Ki67$^+$ subsets, also increased (Figure 5B
313 and Figure 5-figure supplement 1A). These effects were not observed for mice that received
314 *Ifng*$^{-/-}$ NK cells (Figure 5B). CD8$^+$ T cells in a tumor microenvironment (TME) are known to
315 display a complex composition comprising subsets of different activation/differentiation
316 statuses. We categorized lung tissue CD8$^+$ T cells according to PD-1 and Lag3 expression
317 (Figure 5-figure supplement 1A), because PD-1 expression is induced by TCR stimulation
318 (Sharpe & Pauken, 2018) and Lag3 is only expressed by exhausted or progenitor-exhausted
319 (PEX) CD8$^+$ T cells (Calagua et al., 2021; Z. Z. Yang et al., 2017). We reasoned that PD-1$^-$
320 Lag3$^-$ CD8$^+$ T cells (Figure 5-figure supplement 1A) are either naïve or at a very early stage
321 of activation, and found that transfer of *Il10*$^{-/-}$, but not WT, NK cells increased the proportion
322 of CD62L$^+$CD44$^+$ and CD62L$^-$CD44$^+$ subsets, while the proportion of CD62L$^-$CD44$^+$ and
323 Ki67$^+$ subsets were lower in mice that received *Ifng*$^{-/-}$ NK cells compared to those in mice
324 that received WT NK cells (Figure 5C). These results indicate that IL-10 of transferred NK
325 cells inhibits activation of naïve CD8$^+$ T cells, whereas IFN-γ of transferred NK cells
326 promotes their effector differentiation and proliferation. We further examined stem cell-like
327 (SCL) CD8$^+$ T cells that are Tim3$^-$ in PD-1^{lo}Lag3$^-$ CD8$^+$ cells (Figure 5-figure supplement
328 1A) (Castiglioni et al., 2023), and detected an increase of total and Ki67$^+$ SCL CD8$^+$ T cells
329 in mice that received WT or *Il10*$^{-/-}$, but not *Ifng*$^{-/-}$, NK cells (Figure 5D). Transfer of *Il10*$^{-/-}$
330 NK cells resulted in a higher level of SCL CD8$^+$ T cells than when WT NK cells were
331 transferred (Figure 5D). In contrast, NK cell transfer did not alter the proportion of exhausted
332 or PEX CD8$^+$ T cells (Figure 5D and Figure 5-figure supplement 1A). The expression of PD-
333 1, Lag3, Tim3, CD44, CD62L, Ly108 and GrzB by SCL, exhausted, and PEX CD8$^+$ T cells

334 in our analysis is consistent with the known characteristics of these cell populations (Figure
335 5-figure supplement 1B) (Andreatta et al., 2021; Castiglioni et al., 2023; Martinez-Usatorre et
336 al., 2020). Thus, overall, transfer of the IL-15/IL-12-conditioned syngeneic NK cells
337 augmented the activation of cDC1s and cDC2s, as well as the levels and activation of $Foxp3^-$
338 $CD4^+$ T cells, naïve $CD8^+$ T cells and SCL $CD8^+$ T cells in metastatic lungs. Moreover, IFN-
339 γ of the transferred NK cells significantly contributes to these effects.

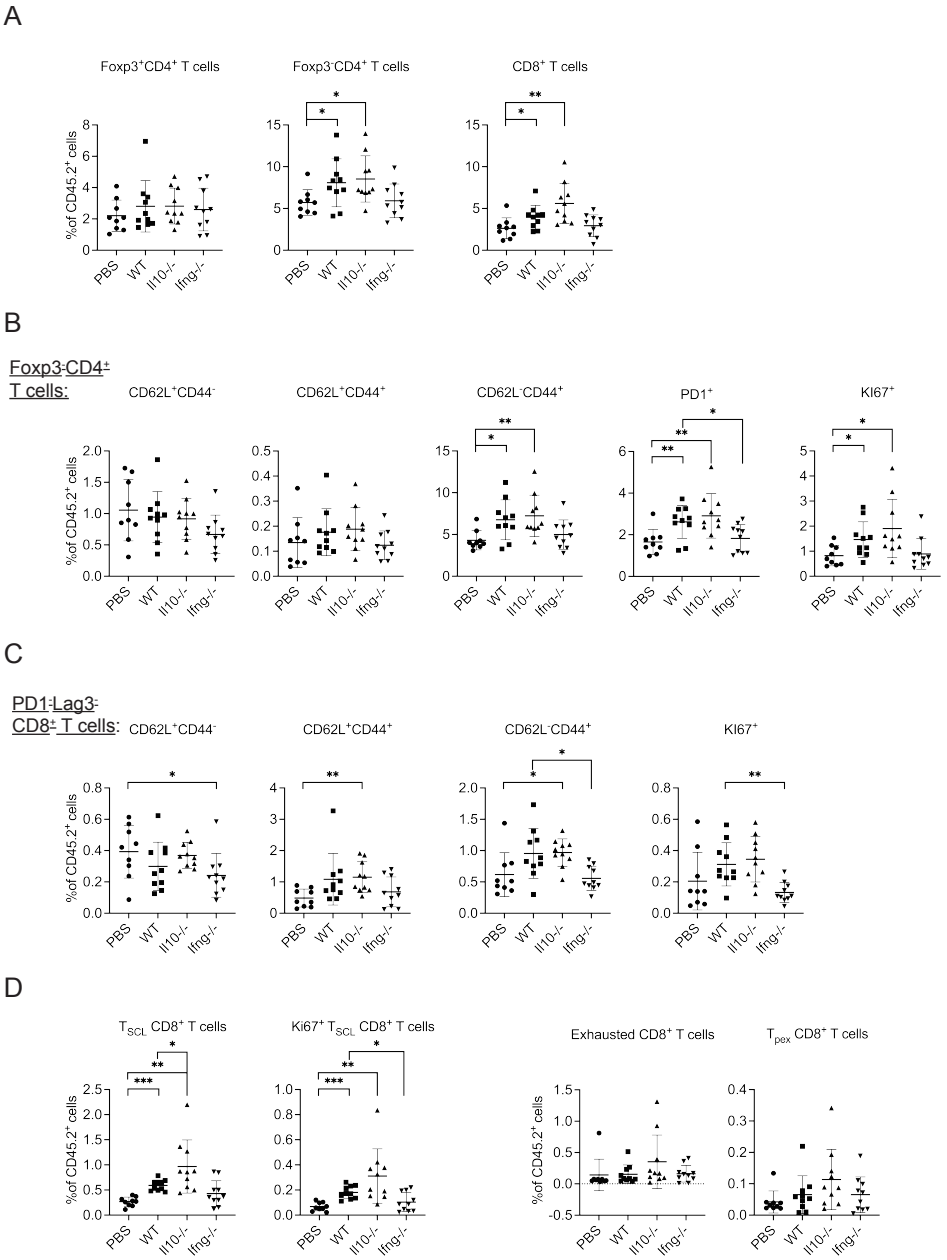

Figure 5. Syngeneic NK cell transfer promotes T cell activation in metastatic lungs.

The experimental design is the same as Figure 4. The proportion of T cell subsets in $CD45^+$ cells in lung tissue were analyzed (Figure 5-figure supplement 1). (A) $Foxp3^+CD4^+$, $Foxp3^-CD4^+$ and $CD8^+$ T cells. (B) $Foxp3^-CD4^+$ T cell subsets. (C) $PD1^-Lag3^-CD8^+$ subsets. (D) Total and $KI67^+$ SCL, exhausted, and PEX $CD8^+$ T cells. Data are compiled from two independent experiments and are presented as mean ± SEM. Each symbol represents one mouse. Statistical significance was determined by unpaired two-tailed Student's t-test: *P≤0.05, **P≤0.01, ***P≤0.001.

Figure supplement 1. Analysis of T cells in lung tissue (related to Figure 5).

350 It is known that CCR7 mediates migration of cDC from tumor to its draining LN (dLN)
351 (Riol-Blanco et al., 2005), in which the migratory cDCs prime tumor-specific naive T cells
352 (Mempel, Henrickson, & von Andrian, 2004). As transfer of WT NK cells increased the
353 levels of $CCR7^{+}LAPM3^{+}MHC\text{-}II^{hi}$ cDC1s and cDC2 in metastatic lungs (Figure 4), we
354 hypothesized that NK cell transfer augments migration of lung cDCs to mLN and activation
355 of T cells. We analyzed migratory and resident cDCs in mLN (Figure 6-figure supplement 1),
356 and found that > 90% of migratory cDC1s and > 65% of migratory cDC2s express CCR7 and
357 LAMP3 (Figure 6A), a phenotype similar to lung $CCR7^{+}LAMP3^{+}MHC\text{-}II^{hi}$ cDC1 and cDC2.
358 On the other hand, the great majority of resident cDC1s and cDC2s in mLN are $CCR7^{-}$
359 $LAMP3^{-}$ (Figure 6A). Transfer of WT NK cells increased the proportion of migratory cDC1
360 in cDCs and the level of CD86 expression by both migratory cDC1s and cDC2s, which
361 required IFN-γ of the transferred NK cells (Figure 6B). We also examined T cells in mLN
362 and found that NK cell transfer affected neither the proportion nor the activation marked by
363 $CD44^{+}$ or $KI67^{+}$ of $Foxp3^{-}CD4^{+}$ and $CD8^{+}$ T cells (data not show). Collectively, NK cell
364 transfer increased the level of migratory cDC1 and CD86 expression by migratory cDC1s and
365 cDC2s, but did not affect T cell activation in mLN.

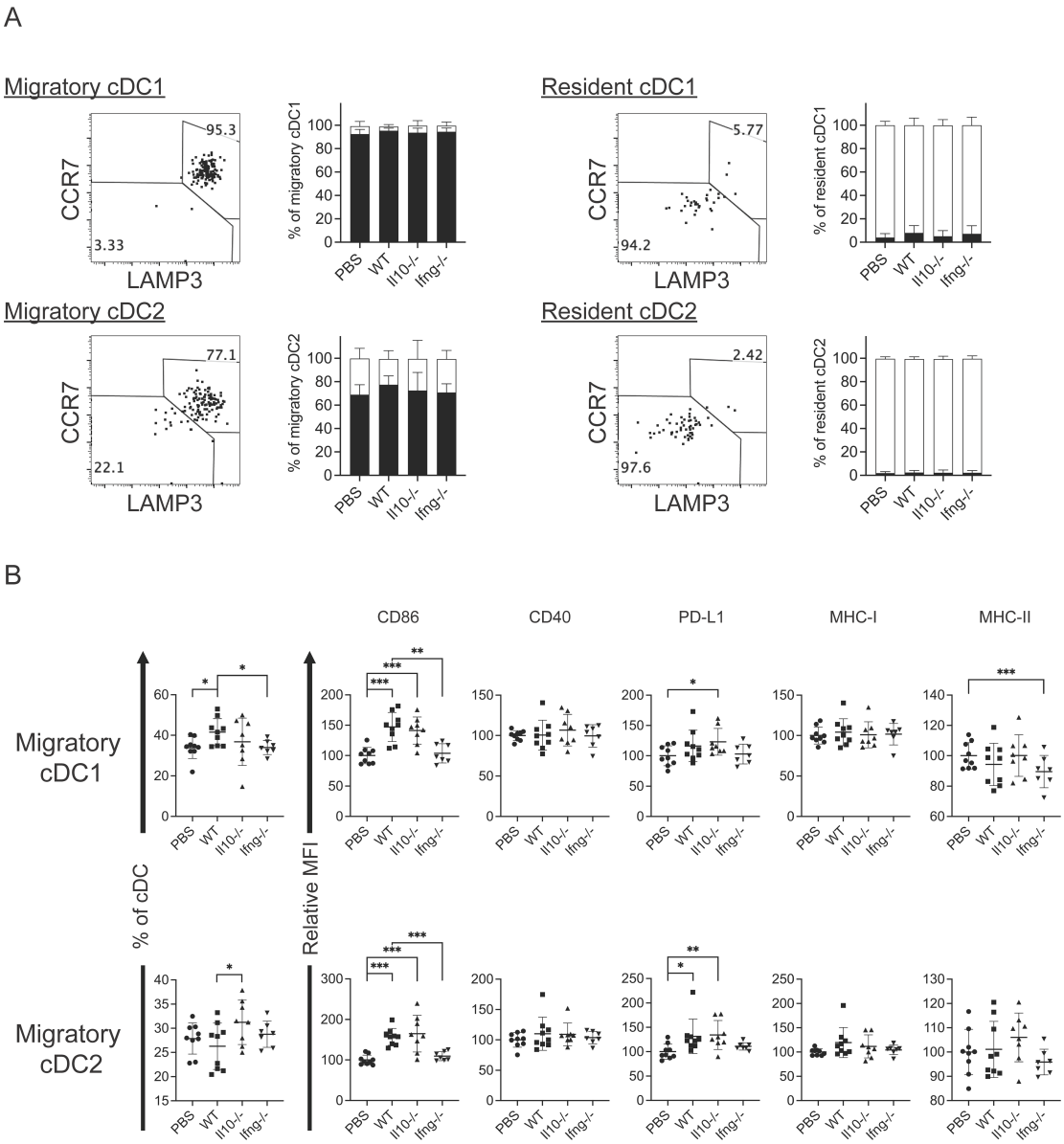

Figure 6. Syngeneic NK cell transfer affects migratory cDCs in mLN.
The experimental design is the same as Fig. 4. (A) The expression of CCR7 and LAMP3 by migratory and resident cDC1s and cDC2s. (B) NK cell transfer affected migratory cDC subsets. The proportion of migratory cDC1s and cDC2s in cDC are shown. The expression of the indicated APC function molecules was analyzed as relative MFI, based on normalization against the mean MFI of the PBS group in each independent experiment. Data are compiled from two independent experiments and presented as mean ± SEM. Each symbol represents one mouse. Statistical significance was determined by unpaired two-tailed Student's t-test: *P≤0.05, **P≤0.01, ***P≤0.001.
Figure supplement 1. Analysis of cDCs in mLN.

377 **Clinical trial of autologous NK cell therapy on advanced cancer patients**

378 To assess NK cell therapy in human, we expanded human NK cells from TCRβ$^-$CD19$^-$
379 PBMCs. The expanded NK cells are identifiable as CD3$^-$CD19$^-$CD14$^-$CD56$^+$EOMES$^+$, with
380 ~90% of the cells expressing HLA-DR (Figure 7A). Co-culture of the expanded HLA-DR$^+$
381 NK cells with K562, THP-1 or U937 tumor cells resulted in dose-dependent tumor cell death
382 (Figure 7B) and increased IFN-γ production by the NK cells (Figure 7C). We then conducted
383 an investigator-initiated clinical trial of autologous NK cell therapy in six pre-treated
384 advanced cancer patients enrolled between May 2016 and October 2019. Baseline
385 characteristics of these patients are presented in Table. The patients had an ECOG
386 performance status of 0, a predicted survival of >3 months, and a relatively small target
387 lesion size (6.4-22.7 mm), suggesting relatively low tumor burden. The patients in cohort 1
388 and cohort 2 received six bi-weekly infusions of 20×10^6 or 30×10^6 autologous HLA-DR$^+$ NK
389 cells, respectively. The infused cells were total cells expanded from TCRβ$^-$CD19$^-$ PBMCs, of
390 which median 92.4% (83.2-94.9%) were HLA-DR$^+$ NK cells (Figure 8A and Figure 8-figure
391 supplement 1). The composition of the infused cells differed slightly among patients, but was
392 stable for each patient over the six infusions (Figure 8A). We examined the expression of
393 NKRs, CD16 and CXCR3 on the HLA-DR$^+$ NK cells and determined that it was stable for
394 each patient over six batches of cell preparations, apart from some variation in NKp44 for
395 patient 5 and CXCR3 for patient 4 (Figure 8B and Figure 8-figure supplement 2). Moreover,
396 the HLA-DR$^+$ NK cells expressed the anti-tumor effectors perforin and IFN-γ (Figure 8C and
397 Figure 8-figure supplement 3). All patients completed the course of six infusions. The
398 therapy proved safe and was well-tolerated by all patients, as no treatment-related adverse
399 effect was observed throughout the entire infusion period up to 24 h after the final infusion.
400 We assessed the preliminary impact of this therapeutic approach based on clinical responses
401 and OS, and present the results with a median follow-up of 60.0 months (2.73-60.0). The

402 response and survival timings were counted from the first infusion of NK cells (Figure 8D).
403 We adopted RECIST 1.1 to evaluate responses, except that the baseline target lesions for
404 patients 3, 4 and 5 (Table) were 18%, 36% and 31% smaller than measurable lesions
405 according to RECIST 1.1. All patients were in a stable disease (SD) state at month 1 (i.e., 1
406 week after the second infusion), and completed six infusions by month 2.3. Patients 1, 3 and
407 6 only received NK cell therapy, whereas patients 2, 4 and 5 received additional treatment(s)
408 as indicated. Patient 1 exhibited progressive disease (PD) at month 2.7 and left the trial.
409 Patient 2 displayed SD for 8.2 months, during which a partial response (PR) was detected at
410 month 4.4. She then received maintenance metronomic Endoxan starting from month 8.4, and
411 displayed SD or PR for a further 50 months. Patient 3 displayed SD for 52.7 months. Patient
412 4 exhibited an SD state for 13 months, received Tarceva during months 14.9-18.6, suffered
413 PD at month 18.6 that prompted receipt of other treatments, and ultimately left the trial at
414 month 31.5. Patient 5 presented SD for 9.9 months, and received metronomic Endoxan
415 during months 7.7-13.5, 28.9-33.0, and 43.6-46.1. She underwent ultrasound imaging during
416 months 17.6-54.2 and the results support a continuing SD state. Patient 6 retained an SD state
417 for 36.3 months, and subsequent ultrasound imaging in month 44.5 supports a continuing SD
418 state. In summary, among the four patients with metastatic solid tumors, patients 1 and 4
419 exhibited PD at month 2.7 and 18.6, respectively, leaving the trial at months 2.7 and 31.5,
420 respectively. In contrast, patients 3 and 6, who only received NK cell therapy, exhibited a SD
421 state and both survived for 60 months. The two follicular lymphoma patients (patients 2 and
422 5) who started maintenance Endoxan therapy ~6 months after undergoing the NK-cell
423 therapy have exhibited a SD state and both survived for 60 months. These preliminary results
424 suggest some level of effectiveness for the autologous NK cell therapy, supporting the
425 efficacy of our pre-clinical mouse model.

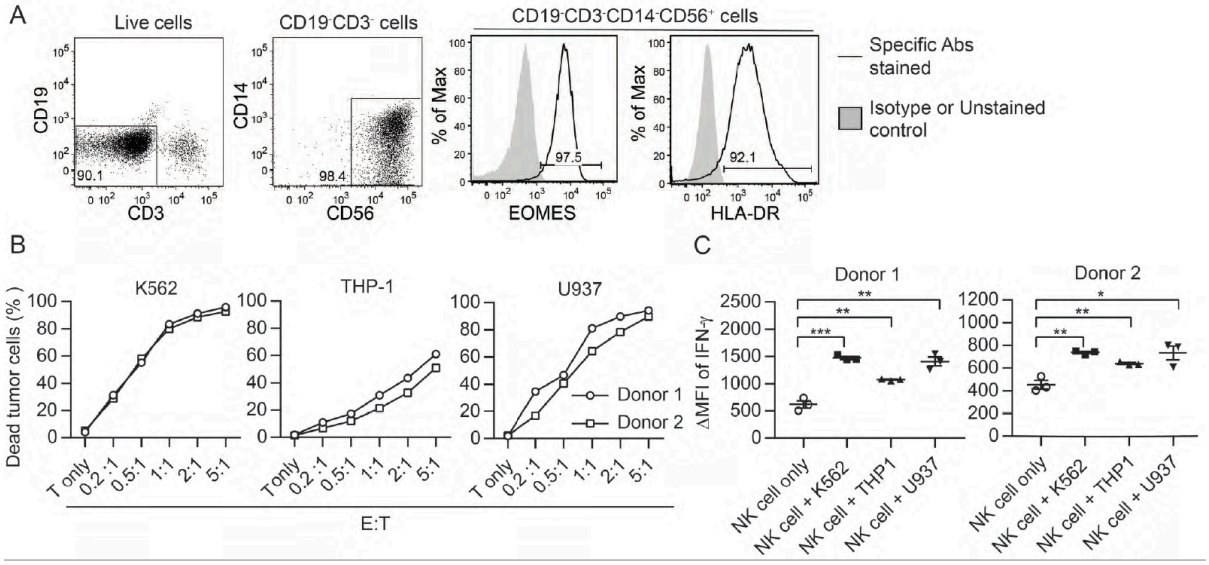

Figure 7. Ex vivo-expanded human NK cells exhibit anti-tumor activities in vitro.

(A) Analysis of expanded human NK cells. Live cells among total cells obtained from human PBMC culture (as described in Methods) were analyzed for the expression of indicated molecules by FACS. Representative plots of 33 healthy donors are shown. (B) Expanded human NK cells kill tumor cells in vitro. Sorted HLA-DR$^+$ NK cells from two healthy donors were co-cultured with CFSE-labeled tumor cells at the indicated E:T ratio. Percentage of dead tumor cells represents the mean ± SEM of PI$^+$ cells among CFSE$^+$ tumor cells from triplicate wells. (C) Expanded human NK cells up-regulate IFN-γ production in response to tumor cells in vitro. Sorted HLA-DR$^+$ NK cells from two healthy donors were co-cultured with tumor cells at a 1:1 ratio for 5 h. Levels of IFN-γ in NK cells were examined by intracellular staining and are calculated as the ΔMFI ± SEM between specific antibody-stained and isotype control antibody-stained samples. Statistical significance was determined by unpaired two-tailed Student's t-test: *P<0.05, **P<0.01, ***P<0.001 relative to NK cells only.

Table. Baseline characteristics of the patients enrolled in the phase I trial.

Characteristic	Cohort 1			Cohort 2		
Patient	1	2	3	4	5	6
Age	63	42	59	66	54	65
Gender	Male	Female	Female	Female	Female	Male
Primary cancer	Colon	Follicular lymphoma	Lung	Lung	Follicular lymphoma	Bladder
Metastasis	Adrenal Lung Pelvis		Lung	Brain		Bone
Previous therapies for cancer						
Surgery	Yes	No	Yes	Yes	No	Yes
Radiotherapy	No	No	No	Yes	No	No
Lines of chemo- or targeted therapy	1	3	0	3	2	4
Immunotherapy	No	No	No	No	No	Keytruda[a]
ECOG performance status	0	0	0	0	0	0
Target lesion (mm)	Pelvic LN (16.3)	Left inguinal LN (18.4)	Mediastinal LN (12.3)	Lung left upper lobe (6.4)	Left axillary LN (10.4)	Pelvic LN (22.7)

a: Ended 7 months before NK cell therapy

439

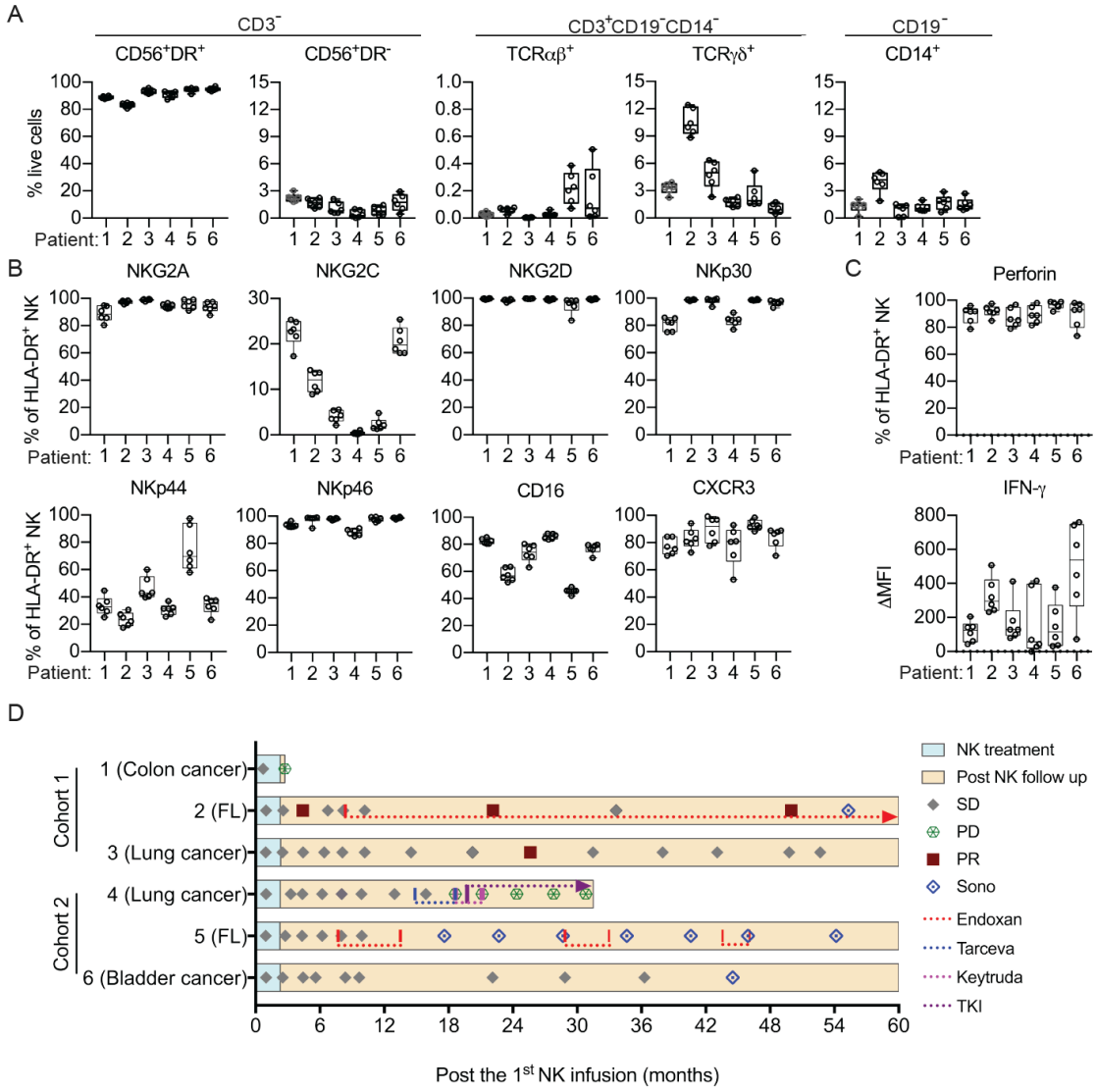

Figure 8. Clinical outcomes of autologous NK cell therapy.

(A) Composition of the infused cells for each patient over six batches of cell preparation. Expression of (B) NKRs, CD16 and CXCR3 and (C) perforin and IFN-γ by the expanded HLA-DR$^+$ NK cells over six batches of cell preparation. Each dot represents a batch of cell preparation. (D) Clinical responses and survival of the six patients. The blue and yellow blocks represent the durations of NK cell treatment and subsequent follow-up, respectively. The response of patients (SD, PD or PR) was evaluated by CT imaging according to RECIST 1.1. Sono symbol marks follow-up using ultrasound imaging. Colored dotted lines indicate the timeframes for additional medications.

Figure supplement 1. Expression of CD56 and HLA-DR by CD3$^-$CD19$^-$CD14$^-$ cells after *ex vivo* expansion (related to Figure 6A).

Figure supplement 2. Expression of NKRs, CD16 and CXCR3 by the expanded HLA-DR$^+$ NK cells.

Figure supplement 3. Expression of IFN-γ and perforin in the expanded HLA-DR$^+$ NK cells.

454 **Discussion**

455

456 The limited benefit achieved with adoptive autologous NK cell therapy for metastatic solid
457 tumors is paradoxical given the clear anti-tumor functions of endogenous NK cells. In this
458 study, we found that transfer of syngeneic NK cells conditioned using IL-15 and IL-12 after
459 resecting the primary tumor resulted in long-term survival of mice with low burden lung
460 metastases. Our results indicate a requirement for $CD8^+$ T cells and the contribution of $CD4^+$
461 T cells to the effectiveness of this NK cell therapy (Figure 3D), which is distinct from the T-
462 cell-independent anti-metastasis mechanisms of NK cells demonstrated previously (Correia et
463 al., 2021; Malladi et al., 2016; Mittal et al., 2017; Takeda et al., 2011; Uemura et al., 2010).
464 The difference in T cell dependency likely arises from differences in experimental design.
465 These previous studies examined the effect of endogenous NK cells on experimental
466 metastasis following intravenous or intrasplenic tumor cell injection by enumerating
467 metastases of affected organs 14 days later. Given that the effect of NK cells on experimental
468 metastasis is mediated by clearing intraluminal tumor cells in microvessels before they
469 extravasate into the target tissue (Spiegel et al., 2016), these studies assessed T cell-
470 independent control of metastasis by NK cells. In contrast, our study examined the effect of
471 adoptively transferred ex vivo-stimulated NK cells on spontaneous metastasis by measuring
472 long-term survival, in which lung metastases were established before primary tumor resection
473 and NK cell administration (Figure 2A). The T cell dependency of the NK cell therapy in our
474 model indicates that innate mechanisms are not sufficient to support the long-term survival of
475 mice with EO771 metastases, which is consistent with the finding from experimental
476 metastasis models that NK cells alone cannot reduce metastases after tumor cells have seeded
477 the target tissue (Spiegel et al., 2016). Importantly, the timeframe we adopted for measuring
478 long-term survival covers the period for the innate effect of the transferred NK cells and the

479 effect of a full T cell response with memory. The $CD8^+$ T cell dependency implies that the
480 transferred NK cells act as an upstream controller for an effective anti-tumor T cell response,
481 which is in line with a previous study showing that early intratumoral accumulation of IFN-γ-
482 producing endogenous NK cells is required for $CD8^+$ T cell-mediated eradication of *Cox*-
483 deficient melanoma in immunocompetent wild-type mice (Bonavita et al., 2020).
484
485 In studying the mechanism underlying T cell-dependency for the effectiveness of NK cell
486 therapy, our results from a mouse model reveal that transfer of WT NK cells augments
487 activation of cDC1s and cDC2s in the metastatic lung (Figure 4). cDC1s and cDC2s present
488 cell-associated and soluble antigens, respectively, to $CD4^+$ and $CD8^+$ T cells (Hildner et al.,
489 2008). The increase of MHC-II^{hi} cDC subsets and elevated expression of MHC-I, MHC-II
490 and CD86 by lung cDC1s and cDC2s presumably promotes T cell activation, which is
491 consistent with the increase of activated lung $Foxp3^-CD4^+$ and $CD8^+$ T cells (Figure 5).
492 Moreover, the elevated CD40 expression by cDC1 and $CD4^+$ T cell activation implies cDC1-
493 relayed $CD4^+$ T cell help for $CD8^+$ T cell response in the lung (Ferris et al., 2020). We also
494 detected an increase of SCL $CD8^+$ T cells in metastatic lungs upon NK cell transfer (Figure
495 5D). Intratumoral tumor-specific SCL $CD8^+$ T cells are known to mediate the responses to
496 PD-1/PD-L1 blockade and adoptive T cell immunotherapies (Krishna et al., 2020; Siddiqui et
497 al., 2019) and are supplied from a reservoir of precursors in the tumor dLN (Connolly et al.,
498 2021; Schenkel et al., 2021). As cDC1s in tumor dLN maintain the SCL $CD8^+$ T cell
499 precursor reservoir (Schenkel et al., 2021), the increase of migratory cDC1 in mLN upon NK
500 cell transfer (Figure 6B) likely contribute to the increase of lung SCL $CD8^+$ T cells.
501 Moreover, a recent study reported that the SCL $CD8^+$ T cell precursors are activated by
502 tumor antigens in the tumor dLN and acquire a stem-like state without an effector phenotype
503 (Prokhnevska et al., 2023). After migrating to a tumor, they differentiate from SCL to an

504 effector state, which requires costimulation by CD80 and CD86 of APC in the TME
505 (Prokhnevska et al., 2023). Our findings of augmented CD86 expression by cDCs and
506 increased proliferating SCL $CD8^+$ T cells in response to NK-cell transfer in metastatic lung
507 are in line with the two-step activation of intratumoral SCL $CD8^+$ T cells. Together, these
508 results demonstrate a clear association between the activation of lung cDCs and T cells in
509 response to NK cell transfer. Furthermore, IFN-γ of transferred NK cells is essential for the
510 augmented activation of both cDCs and T cells, strengthening evidence for the scenario that
511 NK cells activate cDCs and then cDCs activate T cells. The requirement for IFN-γ of
512 transferred NK cells also suggests a direct interaction between transferred NK cells and lung
513 cDCs, which is supported by the increase of $CCR7^+LAMP3^+$ MHC-II^{hi} lung cDCs according
514 to a recent study reporting colocalization of $LAMP3^+$ DCs with NK cells in four types of
515 human solid tumor (Tang et al., 2023). Moreover, this result indicates that NK-cell-derived
516 IFN-γ drives the generation of mregDCs. However, although *Ifng*$^{-/-}$ NK cells induced less
517 cDC activation compared to WT NK cells, the levels of CD86 on cDCs of mice that received
518 *Ifng*$^{-/-}$ NK cells were higher than those of mice not subjected to NK cell transfer (Figure 4B).
519 This outcome indicates the presence of IFN-γ-independent or/and compensatory
520 mechanism(s) for cDC activation by the transferred NK cells, which is in line with our
521 preliminary result that *Ifng*$^{-/-}$ NK cell therapy does not significantly diminish the pro-survival
522 effect in comparison to WT NK cell therapy beyond 60 days after tumor cell inoculation
523 (data not shown).
524
525 IFN-γ is known to upregulate the expression of PD-L1 (Blank et al., 2004). Here, we found
526 that IFN-γ of transferred NK cells augments the level of PD-L1 on cDCs, and the proportion
527 of mregDCs that express the highest level of PD-L1 among lung cDC subsets (Figure 4). PD-
528 L1 is a ligand for the inhibitory PD-1 receptor that induces Treg cell expansion and inhibits

529 CTL cytotoxicity (Arasanz et al., 2017; Dong et al., 2020). A previous study found that PD-
530 L1 on DCs inhibits T cell activation (Peng et al., 2020). Blockade of the PD-L1/PD-1 axis not
531 only promotes activation of tumor-infiltrating $CD8^+$ T cells that leads to tumor control, but
532 also improves the number and functionality of SCL $CD8^+$ T cells within tumors (Castiglioni
533 et al., 2023; Peng et al., 2020; Siddiqui et al., 2019). Additionally, a recent study
534 demonstrated that transfer of NK cells isolated from the spleens of 7-week-old mice,
535 combined with anti-PD-L1 treatment, restored the anti-tumor effect of anti-PD-L1 in aged
536 mice of the MC38 tumor model (Hou et al., 2024). Collectively, we speculate that a
537 combination of adoptive NK cell therapy plus PD-L1 blockade could enhance the
538 effectiveness of cancer treatments.
539
540 In summary, our results indicate that syngeneic IL-15/IL-12-conditioned NK cell therapy
541 promotes tumor-specific T cell responses, at least in part, through activation of cDC1s and
542 cDC2s in metastatic lung. Our findings are consistent with the critical role of endogenous NK
543 cells and $CD8^+$ T cells in anti-tumor immunity, and support that autologous NK cell therapy
544 is effective in treating established low burden MHC-I^+ metastases by enhancing the tumor-
545 specific $CD8^+$ T cell response.
546
547
548 **Materials and Methods**
549
550 **Mice and cell lines**
551 Female C57BL/6JNarl mice (National Laboratory Animal Center of Taiwan, Taipei, Taiwan),
552 *eGFP* transgenic C57BL/6JNarl mice (a gift from Chin-Yen Tsai at Academia Sinica (AS)),
553 *Ifng*$^{-/-}$ mice (strain # 002287, The Jackson Laboratory, Bar Harbor, ME, USA) and *Il10*$^{-/-}$

554 mice (Strain # 002251, The Jackson Laboratory) were housed in a specific pathogen-free
555 animal facility at the Institute of Molecular Biology. Mice aged 8-12 weeks old were used for
556 experiments, unless stated otherwise. All animal protocols were approved by the IACUC of
557 AS. EO771 (CH3 Biosystems), K562 (a gift from Che-Kun James Shen at AS), THP-1 and
558 U937 (gifts from Li-Chung Hsu at National Taiwan University) cells were cultured in RPMI-
559 1640 (Gibco, Grand Island, NY, USA) containing 10% FBS (Hyclone, Marlborough, MA,
560 USA), 20 mM HEPES (Sigma-Aldrich, St. Louis, MO, USA), 100 U/ml penicillin and 100
561 μg/ml streptomycin (Gibco). B16F10 melanoma (a gift from Steve Roffler at AS) was
562 cultured in DMEM (Gibco) containing 10% FBS and 100 U/ml penicillin and 100 μg/ml
563 streptomycin.
564
565 **Flow cytometry**
566 To stain cell surface molecules, cells were incubated with fluorophore-conjugated antibodies
567 for 15 min at 4 °C and washed twice with staining buffer (PBS containing 2% FBS, 5 mM
568 EDTA and 0.01% NaN_3). For staining of intracellular molecules, cells were fixed for 30 min
569 at 4 °C after surface staining with 4% paraformaldehyde, or with a Foxp3/Transcription
570 Factor Fixation/Permeabilization Concentrate and Diluent kit (Thermo Fisher Scientific,
571 Waltham, MA, USA) to stain transcription factors. The fixed cells were then washed with
572 staining buffer, permeabilized with 0.1% saponin, and stained with antibody for 30 min at 4
573 °C. Cells were analyzed by LSRII, FACSymphony A3 or FACSCalibur (BD Biosciences,
574 Franklin Lakes, NJ, USA) and the data were analyzed using FlowJo (BD Biosciences). The
575 antibodies used are detailed in the supplementary materials.
576
577 **Ex vivo expansion of murine and human NK cells**
578 Murine bone marrow (BM) cells were depleted of red blood cells (RBCs) by means of

579 ammonium-chloride-potassium (ACK) buffer (150 mM NH_4Cl, 10 mM $NaHCO_3$, 1 mM
580 EDTA) and then cultured in RPMI-1640 containing 10% FBS (Corning, Corning, NY, USA),
581 20 mM HEPES (Sigma-Aldrich), 200 U/ml penicillin, 200 μg/ml streptomycin (Gibco), 50
582 μg/ml gentamycin (Sigma-Aldrich), 0.2 mg/ml L-glutamine (Sigma-Aldrich), and 50 μM 2-
583 mercaptoethanol (Merck, Rahway, NJ, USA) in a 5% CO_2 incubator at 37 °C for 7 days with
584 30 ng/ml IL-15 (BioLegend, San Diego, CA, USA) and 10 ng/ml IL-12 (Peprotech, Cranbury,
585 NJ, USA). The expanded murine NK cells ($CD19^-TCR\beta^-NK1.1^+CD11c^+B220^+$) were sorted
586 using SORP (BD Biosciences). We used BM cells instead of splenocytes for NK cell culture
587 because removal of T cells from BM cells before culturing is not necessary. Human NK cells
588 were expanded from peripheral blood mononuclear cells (PBMCs) after depleting $TCR\beta^+$ and
589 $CD19^+$ cells with anti-TCRβ (WT31, BD Biosciences) and anti-CD19 (4G7, BD Biosciences)
590 antibodies, and anti-mouse IgG1 microbeads (Miltenyi Biotec, Bergisch Gladbach, Germany)
591 using an LD column with a QuadroMACS Separator (Miltenyi Biotec) under good tissue
592 practice (GTP) conditions. The resulting $TCR\beta^-CD19^-$ PBMCs were cultured in RPMI-1640
593 containing autologous plasma, 20 mM HEPES (Sigma-Aldrich), 2 mM L-glutamine (Cellgro,
594 Lincoln, NE, USA), and 50 μg/ml gentamycin (Winston Medical Supply Co. Ltd.) in a 5%
595 CO_2 incubator at 37 °C for 7 days with 25 ng/ml IL-15 (CellGenix, Freiburg, Germany) and
596 10 ng/ml IL-12 (BioLegend) (Lee & Liao, 2015).
597
598 **In vitro anti-tumor activity of expanded NK cells**
599 Tumor cells were labeled using a Vybrant CFDA SE (CFSE) cell tracer kit (Invitrogen,
600 Waltham, MA, USA). For cytotoxicity assay, sorted NK cells were co-cultured with 10^5
601 labeled tumor cells at the indicated ratio and then incubated for 5 h in a 5% CO_2 incubator at
602 37 °C. The cells were then stained with propidium iodide (PI) and the $CFSE^+$ tumor cells
603 were analyzed for PI^- cells using a LSRII system. For IFN-γ production, sorted NK cells were

604 co-cultured with CFSE-labeled tumor cells at a 1-to-1 ratio, with 10 μg/ml brefeldin A being
605 present for the last 4 h of the co-culture. Cells were then stained intracellularly with anti-IFN-
606 γ or isotype control antibody to detect IFN-γ production by $CFSE^-$ NK cells using a LSRII
607 system.
608
609 **Trafficking of ex vivo-expanded murine NK cells**
610 NK cells expanded from the BM cells of *eGFP* transgenic mice were sorted and
611 intravenously transferred into C57BL/6JNarl mice (6 million cells/mouse) 3 days after
612 resection of a day-21 tumor. Single cell suspensions were prepared from the lung and spleen
613 at the indicated hours after NK cell transfer and analyzed for $eGFP^+$ donor cells using a
614 LSRII system.
615
616 **Gene expression**
617 Lung RNA was extracted using Trizol (Invitrogen) and reverse-transcribed into cDNA using
618 a Reverse Transcription Kit (SMOBIO, Paramount, California, USA). Relative gene
619 expression was determined using a QuantStudio 12K Flex Real-Time PCR system (Thermo
620 Fisher Scientific) with SYBR Green and relative standard curves normalized against
621 expression of cyclophilin a (*Cypa*). The sequences of primers used are detailed in the
622 supplementary materials.
623
624 **EO771 resection and metastasis model and NK cell treatment**
625 Each mouse was inoculated with 0.3 million EO771 cells into the right fourth mammary fat
626 pad on day 0. Twenty-one days later, mice were anesthetized and the resulting tumor and
627 sentinel LN (right inguinal LN) were resected. Sham control mice received the same surgical
628 procedure without removing any tissue. Mice harboring a day-21 tumor weight of <95 mg

629 were excluded since resection alone promoted long-term survival of mice with such tumors.
630 Mice were grouped to have a similar mean and standard deviation of day-21 tumor weight.
631 Each mouse then received 0.3 million expanded NK cells or PBS (Control) via the tail vein
632 three times on days 24, 28 and 31, or once on day 24 as indicated. The resulting metastatic
633 foci on lung surfaces were visualized by staining the dissected lung with India ink under a
634 dissecting microscope. The area of metastatic foci was determined using ImageJ (NIH). For T
635 cell depletion, mice were administered intraperitoneally with 200 μg of anti-CD4 (GK1.5,
636 BioXcell, Lebanon, NH, USA), anti-CD8α (2.43, BioXcell), or both antibodies 19 days after
637 EO771 inoculation, whereas control mice each received 400 μg of isotype control antibody
638 (Rat IgG2b, κ; BioXcell). The mice underwent tumor resection 2 days later, before receiving
639 NK cells as described in the previous section.
640
641 **Isolation of murine T cells and non-T cells**
642 Single cell suspensions were prepared from the BM, spleen, and LNs of NK cell-treated and
643 tumor-rechallenged long-term survivors and from the same tissues of age-matched naïve
644 mice. After lysis of RBCs with ACK buffer, T cells and non-T cells were isolated using Pan
645 T cell isolation Kit II (Miltenyi Biotec) via an autoMACS Pro Separator (Miltenyi Biotec)
646 according to the manufacturer's instructions. The T cell preparations comprised 88-93% of
647 $CD3^+$ cells, and the non-T cell preparations comprised 90-96% of $CD3^-$ cells.
648
649 **Preparation of lung cell suspension**
650 Each mouse received an intravenous injection of 3 μg of FITC-anti-CD45 antibody three
651 minutes before euthanasia to label blood $CD45^+$ cells. Lungs were harvested, minced and
652 washed with PBS to remove excess anti-CD45 antibody. The tissue pieces were digested with
653 0.2 μg/ml of collagenase IV in HBSS (Sigma H1641) containing 2% FBS and 10mM HEPES

654 for 30 min at 37°C with shaking at 200 rpm. RBCs in the lung cell suspension were lysed
655 using ACK lysis buffer.
656
657 **Clinical trial design**
658 We conducted an investigator-driven, open-label, 3+3 design trial to investigate the safety of
659 the autologous NK cell therapy on metastatic/refractory stage IV cancer patients at a single
660 center (ClinicalTrials.gov Identifier: NCT02661685). All six patients were ineligible for or
661 refused further systemic chemotherapy or immunotherapy, and had an Eastern Cooperative
662 Oncology Group (ECOG) performance status of 0, a target lesion, and adequate organ
663 function at the time of enrollment. The three patients in cohort 1 received six bi-weekly
664 intravenous infusions of 20×10^6 expanded autologous HLA-DR$^+$ NK cells, whereas the three
665 patients in cohort 2 were administered with 30×10^6 of the same cells. All patients underwent
666 a computerized tomography (CT) scan between the second and the third NK cell infusions,
667 and then five further CT scans at 8-week intervals starting one week after the sixth infusion.
668 Thereafter, CT or sonography scans were performed as indicated. Safety was evaluated by
669 assessing dose-limiting toxicity (DLT), defined as any treatment-related toxicity of grade 3 or
670 above of general or immune disorders according to the National Cancer Institute-Common
671 Terminology Criteria for Adverse Events (NCI-CTCAE) v4.03. Fever, chills, flu-like
672 symptoms, or infusion-related reactions of grade 3 or above were considered DLT only if
673 they remained at grade 3 or above for more than 3 days despite appropriate medication.
674 Clinical responses to the therapy were evaluated by CT scans according to Response
675 Evaluation Criteria in Solid Tumors version 1.1 (RECIST 1.1). Patient survival was followed
676 every 8 weeks for the first year and every 12 weeks from the second to the fifth year.
677
678 **Trial oversight**

679 The protocols for our clinical trial and follow-up were approved by the Institutional Review
680 Boards (IRBs) at Tri-Service General Hospital and at AS, and were conducted according to
681 the principles of the Declaration of Helsinki. Written informed consent was obtained from all
682 patients.
683
684 **Statistical analysis**
685 Results are presented as mean ± SEM. Statistical significance of in vitro cytotoxicity was
686 examined by unpaired two-tailed Student's t-test. Correlation was determined by Pearson
687 correlation coefficient. The Kaplan-Meier estimator was employed for survival analysis, and
688 statistical significance was determined by a Log-Rank test. Tumor volume was calculated
689 using the formula: length x width^2 x 0.52. Mice with a tumor volume exceeding 2000 mm^3
690 were considered moribund. All statistical analyses were performed using GraphPad Prism 7
691 (GraphPad). ns, not significant; *P<0.05; **P<0.01; ***P<0.001; ****P<0.0001.
692
693
694 **Acknowledgments**
695 We thank the FACS Core and Animal Facilities at the Institute of Molecular Biology, AS, for
696 service and support. We thank Dr. Chee-Jen Chang at the Graduate Institute of Clinical
697 Medical Science, Chang Gung University, for consultation on statistical design of the clinical
698 trial. We thank Ms. Yi-Min Liu and colleagues at the Translation Resource Center for
699 Genomic Medicine, Institute of Biomedical Science, AS, for assistance with designing the
700 case report form, the Oracle clinical system and IRB affairs. We thank the Instrument Center
701 at the National Defense Medical Center for flow cytometry services. We thank Dr. John
702 O'Brien for manuscript editing.
703

704

705 **References**

706 Alspach, E., Lussier, D. M., & Schreiber, R. D. (2019). Interferon gamma and Its Important
707 Roles in Promoting and Inhibiting Spontaneous and Therapeutic Cancer Immunity.
708 *Cold Spring Harb Perspect Biol, 11*(3). doi:10.1101/cshperspect.a028480

709 Andreatta, M., Corria-Osorio, J., Muller, S., Cubas, R., Coukos, G., & Carmona, S. J. (2021).
710 Interpretation of T cell states from single-cell transcriptomics data using reference
711 atlases. *Nat Commun, 12*(1), 2965. doi:10.1038/s41467-021-23324-4

712 Arasanz, H., Gato-Canas, M., Zuazo, M., Ibanez-Vea, M., Breckpot, K., Kochan, G., &
713 Escors, D. (2017). PD1 signal transduction pathways in T cells. *Oncotarget, 8*(31),
714 51936-51945. doi:10.18632/oncotarget.17232

715 Barry, K. C., Hsu, J., Broz, M. L., Cueto, F. J., Binnewies, M., Combes, A. J., . . . Krummel,
716 M. F. (2018). A natural killer-dendritic cell axis defines checkpoint therapy-
717 responsive tumor microenvironments. *Nat Med, 24*(8), 1178-1191.
718 doi:10.1038/s41591-018-0085-8

719 Blank, C., Brown, I., Peterson, A. C., Spiotto, M., Iwai, Y., Honjo, T., & Gajewski, T. F.
720 (2004). PD-L1/B7H-1 inhibits the effector phase of tumor rejection by T cell receptor
721 (TCR) transgenic CD8+ T cells. *Cancer Res, 64*(3), 1140-1145. doi:10.1158/0008-
722 5472.can-03-3259

723 Bonavita, E., Bromley, C. P., Jonsson, G., Pelly, V. S., Sahoo, S., Walwyn-Brown, K., . . .
724 Zelenay, S. (2020). Antagonistic inflammatory phenotypes dictate tumor fate and
725 response to immune checkpoint blockade. *Immunity, 53*(6), 1215-1229 e1218.
726 doi:10.1016/j.immuni.2020.10.020

727 Bottcher, J. P., Bonavita, E., Chakravarty, P., Blees, H., Cabeza-Cabrerizo, M., Sammicheli,
728 S., . . . Reis e Sousa, C. (2018). NK Cells Stimulate Recruitment of cDC1 into the

729 Tumor Microenvironment Promoting Cancer Immune Control. *Cell, 172*(5), 1022-
730 1037.e1014. doi:10.1016/j.cell.2018.01.004
731 Cabeza-Cabrerizo, M., Cardoso, A., Minutti, C. M., Pereira da Costa, M., & Reis e Sousa, C.
732 (2021). Dendritic Cells Revisited. *Annu Rev Immunol, 39*, 131-166.
733 doi:10.1146/annurev-immunol-061020-053707
734 Calagua, C., Ficial, M., Jansen, C. S., Hirz, T., Del Balzo, L., Wilkinson, S., . . . Einstein, D.
735 J. (2021). A Subset of Localized Prostate Cancer Displays an Immunogenic
736 Phenotype Associated with Losses of Key Tumor Suppressor Genes. *Clin Cancer Res,*
737 *27*(17), 4836-4847. doi:10.1158/1078-0432.CCR-21-0121
738 Castiglioni, A., Yang, Y., Williams, K., Gogineni, A., Lane, R. S., Wang, A. W., . . . Muller,
739 S. (2023). Combined PD-L1/TGFbeta blockade allows expansion and differentiation
740 of stem cell-like CD8 T cells in immune excluded tumors. *Nat Commun, 14*(1), 4703.
741 doi:10.1038/s41467-023-40398-4
742 Chen, X. H., Liu, Z. C., Zhang, G., Wei, W., Wang, X. X., Wang, H., . . . Du, J. (2015). TGF-
743 beta and EGF induced HLA-I downregulation is associated with epithelial-
744 mesenchymal transition (EMT) through upregulation of snail in prostate cancer cells.
745 *Mol Immunol, 65*(1), 34-42. doi:10.1016/j.molimm.2014.12.017
746 Cheng, S., Li, Z., Gao, R., Xing, B., Gao, Y., Yang, Y., . . . Zhang, Z. (2021). A pan-cancer
747 single-cell transcriptional atlas of tumor infiltrating myeloid cells. *Cell, 184*(3), 792-
748 809 e723. doi:10.1016/j.cell.2021.01.010
749 Chockley, P. J., Chen, J., Chen, G., Beer, D. G., Standiford, T. J., & Keshamouni, V. G.
750 (2018). Epithelial-mesenchymal transition leads to NK cell-mediated metastasis-
751 specific immunosurveillance in lung cancer. *J Clin Invest, 128*(4), 1384-1396.
752 doi:10.1172/JCI97611

753 Connolly, K. A., Kuchroo, M., Venkat, A., Khatun, A., Wang, J. W., William, I., . . . Joshi, N.
754 S. (2021). A reservoir of stem-like CD8 T cells in the tumor-draining lymph node
755 preserves the ongoing antitumor immune response. *Science Immunology, 6*(64).
756 doi:https://doi.org/10.1126/sciimmunol.abg7836
757 Correia, A. L., Guimaraes, J. C., Auf der Maur, P., De Silva, D., Trefny, M. P., Okamoto,
758 R., . . . Bentires-Alj, M. (2021). Hepatic stellate cells suppress NK cell-sustained
759 breast cancer dormancy. *Nature, 594*(7864), 566-571. doi:10.1038/s41586-021-
760 03614-z
761 de Saint-Vis, B., Vincent, J., Vandenabeele, S., Vanbervliet, B., Pin, J. J., Ait-Yahia, S., . . .
762 Lebecque, S. (1998). A novel lysosome-associated membrane glycoprotein, DC-
763 LAMP, induced upon DC maturation, is transiently expressed in MHC class II
764 compartment. *Immunity, 9*(3), 325-336. doi:10.1016/s1074-7613(00)80615-9
765 Dong, Y., Han, Y., Huang, Y., Jiang, S., Huang, Z., Chen, R., . . . Zhang, S. (2020). PD-L1 Is
766 Expressed and Promotes the Expansion of Regulatory T Cells in Acute Myeloid
767 Leukemia. *Front Immunol, 11*, 1710. doi:10.3389/fimmu.2020.01710
768 Ewens, A., Mihich, E., & Ehrke, M. J. (2005). Distant metastasis from subcutaneously grown
769 E0771 medullary breast adenocarcinoma. *Anticancer Res, 25*(6b), 3905-3915.
770 Retrieved from http://ar.iiarjournals.org/content/25/6B/3905.full.pdf
771 Fang, F., Xiao, W., & Tian, Z. (2017). NK cell-based immunotherapy for cancer. *Semin*
772 *Immunol, 31*, 37-54. doi:10.1016/j.smim.2017.07.009
773 Ferris, S. T., Durai, V., Wu, R., Theisen, D. J., Ward, J. P., Bern, M. D., . . . Murphy, K. M.
774 (2020). cDC1 prime and are licensed by CD4(+) T cells to induce anti-tumour
775 immunity. *Nature, 584*(7822), 624-629. doi:10.1038/s41586-020-2611-3

776 Freud, A. G., Mundy-Bosse, B. L., Yu, J., & Caligiuri, M. A. (2017). The Broad Spectrum of
777 Human Natural Killer Cell Diversity. *Immunity, 47*(5), 820-833.
778 doi:10.1016/j.immuni.2017.10.008
779 Ganesh, K., & Massague, J. (2021). Targeting metastatic cancer. *Nat Med, 27*(1), 34-44.
780 doi:10.1038/s41591-020-01195-4
781 Gordon, S. M., Chaix, J., Rupp, L. J., Wu, J., Madera, S., Sun, J. C., . . . Reiner, S. L. (2012).
782 The transcription factors T-bet and Eomes control key checkpoints of natural killer
783 cell maturation. *Immunity, 36*(1), 55-67. doi:10.1016/j.immuni.2011.11.016
784 Hildner, K., Edelson, B. T., Purtha, W. E., Diamond, M., Matsushita, H., Kohyama, M., . . .
785 Murphy, K. M. (2008). Batf3 deficiency reveals a critical role for CD8alpha+
786 dendritic cells in cytotoxic T cell immunity. *Science, 322*(5904), 1097-1100.
787 doi:10.1126/science.1164206
788 Hou, J., Xie, S., Gao, J., Jiang, T., Zhu, E., Yang, X., . . . Wang, X. (2024). NK cell transfer
789 overcomes resistance to PD-(L)1 therapy in aged mice. *Exp Hematol Oncol, 13*(1), 48.
790 doi:10.1186/s40164-024-00511-9
791 Huntington, N. D., Cursons, J., & Rautela, J. (2020). The cancer-natural killer cell immunity
792 cycle. *Nat Rev Cancer, 20*(8), 437-454. doi:10.1038/s41568-020-0272-z
793 Jamieson, A. M., Diefenbach, A., McMahon, C. W., Xiong, N., Carlyle, J. R., & Raulet, D. H.
794 (2002). The role of the NKG2D immunoreceptor in immune cell activation and
795 natural killing. *Immunity, 17*(1), 19-29. doi:10.1016/s1074-7613(02)00333-3
796 Karre, K., Ljunggren, H. G., Piontek, G., & Kiessling, R. (2005). Selective rejection of H-2-
797 deficient lymphoma variants suggests alternative immune defence strategy. 1986. *J*
798 *Immunol, 174*(11), 6566-6569. Retrieved from
799 https://www.ncbi.nlm.nih.gov/pubmed/15905492

800 Kennedy, M. K., Glaccum, M., Brown, S. N., Butz, E. A., Viney, J. L., Embers, M., . . .
801 Peschon, J. J. (2000). Reversible defects in natural killer and memory CD8 T cell
802 lineages in interleukin 15-deficient mice. *J Exp Med, 191*(5), 771-780.
803 doi:10.1084/jem.191.5.771
804 Krishna, S., Lowery, F. J., Copeland, A. R., Bahadiroglu, E., Mukherjee, R., Jia, L., . . .
805 Rosenberg, S. A. (2020). Stem-like CD8 T cells mediate response of adoptive cell
806 immunotherapy against human cancer. *Science, 370*(6522), 1328-1334.
807 doi:10.1126/science.abb9847
808 Lee, J. M., & Liao, N. S. (2015). United States Patent No. 9157068 B2.
809 Lodolce, J. P., Boone, D. L., Chai, S., Swain, R. E., Dassopoulos, T., Trettin, S., & Ma, A.
810 (1998). IL-15 receptor maintains lymphoid homeostasis by supporting lymphocyte
811 homing and proliferation. *Immunity, 9*(5), 669-676. doi:10.1016/s1074-
812 7613(00)80664-0
813 Lopez-Soto, A., Gonzalez, S., Smyth, M. J., & Galluzzi, L. (2017). Control of Metastasis by
814 NK Cells. *Cancer Cell, 32*(2), 135-154. doi:10.1016/j.ccell.2017.06.009
815 Lopez-Soto, A., Huergo-Zapico, L., Galvan, J. A., Rodrigo, L., de Herreros, A. G., Astudillo,
816 A., & Gonzalez, S. (2013). Epithelial-mesenchymal transition induces an antitumor
817 immune response mediated by NKG2D receptor. *J Immunol, 190*(8), 4408-4419.
818 doi:10.4049/jimmunol.1202950
819 Maier, B., Leader, A. M., Chen, S. T., Tung, N., Chang, C., LeBerichel, J., . . . Merad, M.
820 (2020). A conserved dendritic-cell regulatory program limits antitumour immunity.
821 *Nature, 580*(7802), 257-262. doi:10.1038/s41586-020-2134-y
822 Malladi, S., Macalinao, D. G., Jin, X., He, L., Basnet, H., Zou, Y., . . . Massague, J. (2016).
823 Metastatic Latency and Immune Evasion through Autocrine Inhibition of WNT. *Cell,*
824 *165*(1), 45-60. doi:10.1016/j.cell.2016.02.025

825 Marcenaro, E., Della Chiesa, M., Bellora, F., Parolini, S., Millo, R., Moretta, L., & Moretta,
826 A. (2005). IL-12 or IL-4 prime human NK cells to mediate functionally divergent
827 interactions with dendritic cells or tumors. *J Immunol, 174*(7), 3992-3998.
828 doi:10.4049/jimmunol.174.7.3992
829 Martin-Fontecha, A., Thomsen, L. L., Brett, S., Gerard, C., Lipp, M., Lanzavecchia, A., &
830 Sallusto, F. (2004). Induced recruitment of NK cells to lymph nodes provides IFN-
831 gamma for T(H)1 priming. *Nat Immunol, 5*(12), 1260-1265. doi:10.1038/ni1138
832 Martinez-Usatorre, A., Carmona, S. J., Godfroid, C., Yacoub Maroun, C., Labiano, S., &
833 Romero, P. (2020). Enhanced Phenotype Definition for Precision Isolation of
834 Precursor Exhausted Tumor-Infiltrating CD8 T Cells. *Front Immunol, 11*, 340.
835 doi:10.3389/fimmu.2020.00340
836 Melaiu, O., Lucarini, V., Cifaldi, L., & Fruci, D. (2019). Influence of the Tumor
837 Microenvironment on NK Cell Function in Solid Tumors. *Front Immunol, 10*, 3038.
838 doi:10.3389/fimmu.2019.03038
839 Mempel, T. R., Henrickson, S. E., & von Andrian, U. H. (2004). T-cell priming by dendritic
840 cells in lymph nodes occurs in three distinct phases. *Nature, 427*(6970), 154-159.
841 doi:10.1038/nature02238
842 Mittal, D., Vijayan, D., Putz, E. M., Aguilera, A. R., Markey, K. A., Straube, J., . . . Smyth,
843 M. J. (2017). Interleukin-12 from CD103(+) Batf3-dependent dendritic cells required
844 for NK-Cell suppression of metastasis. *Cancer Immunol Res, 5*(12), 1098-1108.
845 doi:10.1158/2326-6066.CIR-17-0341
846 Mocikat, R., Braumuller, H., Gumy, A., Egeter, O., Ziegler, H., Reusch, U., . . . Rocken, M.
847 (2003). Natural killer cells activated by MHC class I(low) targets prime dendritic cells
848 to induce protective CD8 T cell responses. *Immunity, 19*(4), 561-569. Retrieved from
849 https://ac.els-cdn.com/S1074761303002644/1-s2.0-S1074761303002644-

850 main.pdf?_tid=1a97a508-b220-482d-b58b-
851 ff113e2c772d&acdnat=1547709680_420dfea0f64bd7bf375b970454538332
852 Parkhurst, M. R., Riley, J. P., Dudley, M. E., & Rosenberg, S. A. (2011). Adoptive transfer of
853 autologous natural killer cells leads to high levels of circulating natural killer cells but
854 does not mediate tumor regression. *Clin Cancer Res, 17*(19), 6287-6297.
855 doi:https://doi.org/10.1158/1078-0432.CCR-11-1347
856 Peng, Q., Qiu, X., Zhang, Z., Zhang, S., Zhang, Y., Liang, Y., . . . Tang, H. (2020). PD-L1 on
857 dendritic cells attenuates T cell activation and regulates response to immune
858 checkpoint blockade. *Nat Commun, 11*(1), 4835. doi:10.1038/s41467-020-18570-x
859 Prokhnevska, N., Cardenas, M. A., Valanparambil, R. M., Sobierajska, E., Barwick, B. G.,
860 Jansen, C., . . . Kissick, H. (2023). CD8+T cell activation in cancer comprises an
861 initial activation phase in lymph nodes followed by effector differentiation within the
862 tumor. *Immunity, 56*(1), 107-124.e105. doi:10.1016/j.immuni.2022.12.002
863 Raulet, D. H. (2003). Roles of the NKG2D immunoreceptor and its ligands. *Nat Rev Immunol,*
864 *3*(10), 781-790. doi:10.1038/nri1199
865 Riol-Blanco, L., Sánchez-Sánchez, N., Torres, A., Tejedor, A., Narumiya, S., Corbí, A. L., . . .
866 Rodríguez-Fernández, J. L. (2005). The chemokine receptor CCR7 activates in
867 dendritic cells two signaling modules that independently regulate chemotaxis and
868 migratory speed. *Journal of Immunology, 174*(7), 4070-4080. doi:DOI
869 10.4049/jimmunol.174.7.4070
870 Sakamoto, N., Ishikawa, T., Kokura, S., Okayama, T., Oka, K., Ideno, M., . . . Yoshikawa, T.
871 (2015). Phase I clinical trial of autologous NK cell therapy using novel expansion
872 method in patients with advanced digestive cancer. *J Transl Med, 13*, 277.
873 doi:10.1186/s12967-015-0632-8

874 Schenkel, J. M., Herbst, R. H., Canner, D., Li, A., Hillman, M., Shanahan, S. L., . . . Jacks, T.
875 (2021). Conventional type I dendritic cells maintain a reservoir of proliferative tumor-
876 antigen specific TCF-1 CD8 T cells in tumor-draining lymph nodes. *Immunity, 54*(10),
877 2338-2353.e2336. doi:10.1016/j.immuni.2021.08.026
878 Sharpe, A. H., & Pauken, K. E. (2018). The diverse functions of the PD1 inhibitory pathway.
879 *Nat Rev Immunol, 18*(3), 153-167. doi:10.1038/nri.2017.108
880 Siddiqui, I., Schaeuble, K., Chennupati, V., Marraco, S. A. F., Calderon-Copete, S., Ferreira,
881 D. P., . . . Held, W. (2019). Intratumoral Tcf1 PD-1 CD8 T Cells with Stem-like
882 Properties Promote Tumor Control in Response to Vaccination and Checkpoint
883 Blockade Immunotherapy. *Immunity, 50*(1), 195-221.e110.
884 doi:10.1016/j.immuni.2018.12.021
885 Smyth, M. J., Cretney, E., Kelly, J. M., Westwood, J. A., Street, S. E., Yagita, H., . . .
886 Hayakawa, Y. (2005). Activation of NK cell cytotoxicity. *Mol Immunol, 42*(4), 501-
887 510. doi:10.1016/j.molimm.2004.07.034
888 Spiegel, A., Brooks, M. W., Houshyar, S., Reinhardt, F., Ardolino, M., Fessler, E., . . .
889 Weinberg, R. A. (2016). Neutrophils suppress intraluminal NK Cell-mediated tumor
890 cell clearance and enhance extravasation of disseminated carcinoma cells. *Cancer*
891 *Discov, 6*(6), 630-649. doi:10.1158/2159-8290.CD-15-1157
892 Takeda, K., Nakayama, M., Sakaki, M., Hayakawa, Y., Imawari, M., Ogasawara, K., . . .
893 Smyth, M. J. (2011). IFN-gamma production by lung NK cells is critical for the
894 natural resistance to pulmonary metastasis of B16 melanoma in mice. *J Leukoc Biol,*
895 *90*(4), 777-785. doi:10.1189/jlb.0411208
896 Tang, F., Li, J. H., Qi, L., Liu, D. F., Bo, Y. F., Qin, S. S., . . . Zhang, Z. M. (2023). A pan-
897 cancer single-cell panorama of human natural killer cells. *Cell, 186*(19), 4235-
898 4251.e4220. doi:10.1016/j.cell.2023.07.034

899 Thommen, D. S., & Schumacher, T. N. (2018). T Cell Dysfunction in Cancer. *Cancer Cell, 33*(4), 547-562. doi:10.1016/j.ccell.2018.03.012

901 Uemura, A., Takehara, T., Miyagi, T., Suzuki, T., Tatsumi, T., Ohkawa, K., . . . Hayashi, N. (2010). Natural killer cell is a major producer of interferon gamma that is critical for the IL-12-induced anti-tumor effect in mice. *Cancer Immunol Immunother, 59*(3), 453-463. doi:10.1007/s00262-009-0764-x

905 Yang, Y., Yang, H. H., Hu, Y., Watson, P. H., Liu, H. Y., Geiger, T. R., . . . Wakefield, L. M. (2017). Immunocompetent mouse allograft models for development of therapies to target breast cancer metastasis. *Oncotarget, 8*(19), 30621-30643. doi:https://doi.org/10.18632/oncotarget.15695

909 Yang, Z. Z., Kim, H. J., Villasboas, J. C., Chen, Y. P., Price-Troska, T., Jalali, S., . . . Ansell, S. M. (2017). Expression of LAG-3 defines exhaustion of intratumoral PD-1(+) T cells and correlates with poor outcome in follicular lymphoma. *Oncotarget, 8*(37), 61425-61439. doi:10.18632/oncotarget.18251

913